6-2015

Kinetic Modeling of Catalytic Aerogels

Yi Cao
Union College - Schenectady, NY

Kinetic Modeling of Catalytic Aerogels

By

Yi Cao

****

Submitted in partial fulfillment
of the requirements for
Honors in the Departments of
Mechanical Engineering and Chemistry

UNION COLLEGE

June, 2015

Abstract

CAO, YI Kinetic Modeling of Catalytic Aerogels. Departments of Mechanical Engineering and Chemistry, June 2015.

ADVISORS: Professors Ann Anderson and Mary Carroll

As pollution becomes an increasing concern globally, strict regulations have been set on vehicle pollutant emissions. The three-way catalytic converter is capable of converting toxic emissions such as carbon monoxide, unburned hydrocarbons and nitrogen oxides to less hazardous waste such as carbon dioxide, water, and nitrogen. Current catalysts employ platinum group metals, which are expensive and environmentally damaging to mine. Catalytically-active aerogels such as Co-Al, Cu-Al and V-Al aerogels have shown promise as alternatives to these metals.

The work presented here adapts and extends a global kinetic model which predicts the conversion of hydrocarbons and carbon monoxide on platinum catalyst surfaces. In this thesis, the kinetic model was constructed in MATLAB and used to predict conversion of hydrocarbons and carbon monoxide using kinetic parameters for platinum. The predicted conversion values produced a good fit to experimental data for both hydrocarbons and carbon monoxide. This model was then applied to catalytically-active Co-Al aerogels. Oxidation reactions of carbon monoxide and hydrocarbons were simulated using kinetic parameters for platinum. Experimental data collected for catalytically-active Co-Al aerogels was then used to optimize these parameters.

The robustness of a genetic algorithm technique for calculating kinetic parameters was achieved by optimizing all kinetic parameters in the original platinum model based solely on experimental data. The optimized values produced are in very good agreement with literature values for platinum. When applied to experimental data for Co-Al aerogels, the optimized models have a fair agreement. More data relating

conversion to space velocity are needed to provide a better understanding of the specific reaction mechanisms and reaction rates for catalytically-active aerogels. Once these models are able to accurately describe kinetic aspects of catalytic reactions, they will be used to predict catalytic results for Co-Al aerogels for untested experimental conditions.

Acknowledgements

This material is based upon work supported by the National Science Foundation through NSF RUI DMR-1206631 and NSF MRI CBET-1228851. I would like to thank my thesis advisors, Professor Ann Anderson and Professor Mary Carroll, for help, guidance and encouragement throughout this project. I would like to show my gratitude to Professor Andrew Huisman, and to Thomas Berkemeier from the Max Planck Institute for Chemistry in Mainz, Germany, for providing the genetic algorithm method used in the optimization process. In addition, I would like to thank Professor Bradford Bruno for his leadership in developing the catalytic testbed and Isaac Ramphal for obtaining the experimental data and for his support throughout this project. Isaac Ramphal's dedication and rigorous experimental work, and his careful thought and inputs have inspired me in so many ways. The support from the whole aerogel research team is also greatly appreciated.

Table of Contents

List of Tables

List of Figures

1. Introduction

1.1 Automotive Emissions

In the incomplete combustion of gasoline, unburned hydrocarbons (HC), nitrogen oxides (NO_x), and carbon monoxide (CO) are released as pollutants. In the early 1950's, a typical car emitted ca. 8.1 g/km hydrocarbons, 2.2 g/km nitrogen oxides, and 54 g/km carbon monoxide, which led to a significant deterioration of air quality [1]. Due to their negative environmental impact, emission of these pollutants from automotive exhaust has been strictly regulated. The Clean Air Act in 1970 called for a 90% reduction in emissions from new automobiles by 1975, with amendments in subsequent years requiring even stricter emission controls [1]. The 2004 U.S. Exhaust standards for light-duty gasoline-fuel vehicles set the emission limits to ca. 0.077 g/km hydrocarbons, 0.12 g/km nitrogen oxides, and 1.1 g/km carbon monoxide [1].

1. 2 The Catalytic Converter

A variety of methods can be used for exhaust after-treatment, including three-way catalytic converters, selective catalytic reduction (SCR), lean NO_x traps (LNT) and catalyzed soot filters (CSF) [2]. In automotive catalysis, a catalytic converter is located downstream of the engine in the exhaust system. It converts toxic emissions such as CO, HC and NO_x to less hazardous waste such as carbon dioxide (CO_2), water (H_2O), and nitrogen (N_2) gases [3]. A typical catalytic converter consists of a catalyst support, which is most commonly a honeycomb-structured ceramic monolith of cordierite. A washcoat containing catalytic materials is applied on the substrate to maximize the catalytic surface

area [3]. In the automotive industry, platinum group metals (platinum, palladium, and rhodium) are washcoated in a slurry of Al_2O_3 onto cordierite to act as three-way catalysts [4]. A schematic of a three-way converter is shown in Figure 1.1.

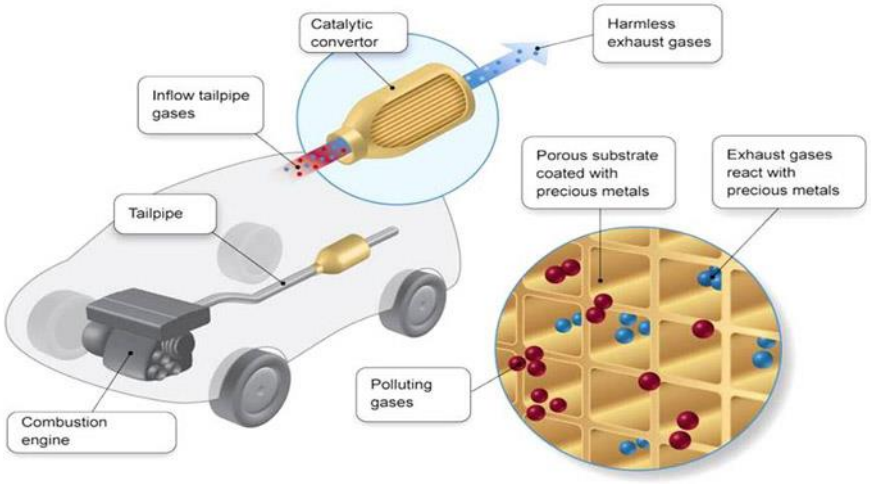

Figure 1.1. Image of a three-way catalytic converter [5].

Various gaseous species flow through the channels of the reactor, diffuse into the washcoat, adsorb onto open catalyst sites, and react chemically at the active sites [6]. Then the products desorb and diffuse back into the exhaust flow [6]. This process involves convective mass transport, species diffusion in the fluid phase, and temperature variation in the monolith due to heat conduction in the fluid and solid wall, convection in the fluid, radiation and chemically generated heat at the wall. The relevant physical and chemical phenomena in the gas phase, washcoat and substrate are summarized in Figure 1.2.

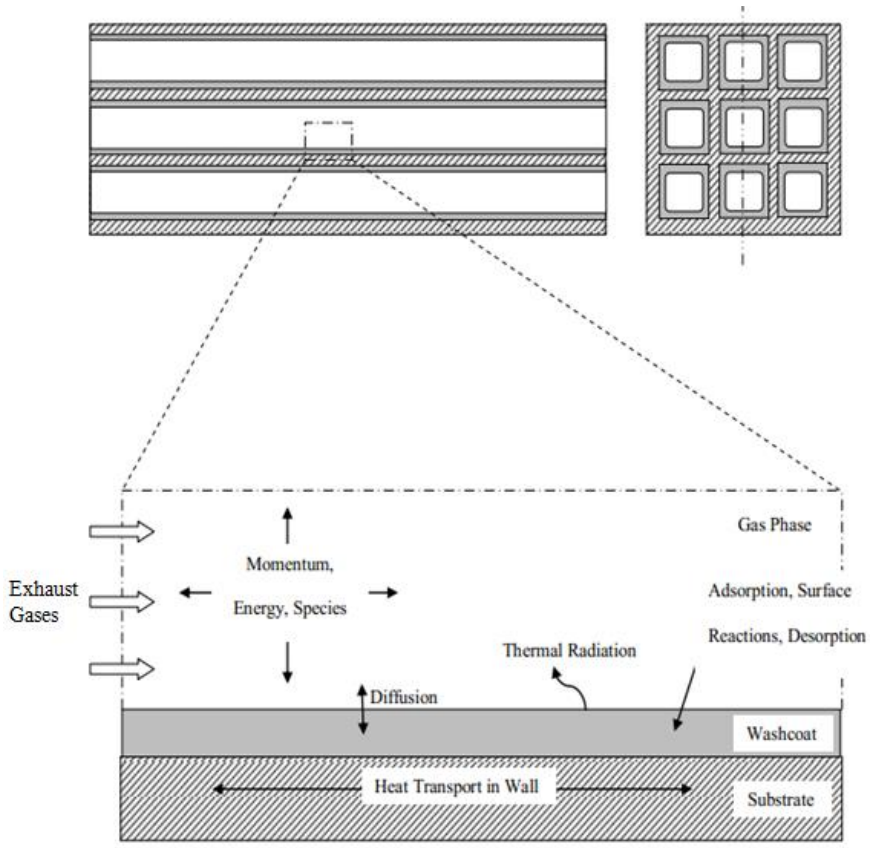

Figure 1.2. Image of physical and chemical phenomena occurred in the monolith channels [6].

1.3 Surface Reactions

The performance of a catalytic converter can be characterized experimentally, which requires a complex experimental facility, or numerically through simulation. There are two major types of models used in the numerical simulation of the catalytic converter: micro-kinetics models and global models. The micro-kinetics models describe the reactions on a molecular level (using a set of quasi-elementary steps). Sub-mechanisms are developed for each reactant and rate constants for each of the elementary reactions are determined by fitting experimental data to proposed models [7]. This detailed chemistry

method enables the prediction of the behavior of the chemical system under any external conditions through extrapolation [8]. However, the current catalytic testing system at the Union College Aerogel Lab does not allow monitoring of intermediate species and thus not enough data are available to develop micro-kinetics models.

Global models, on the other hand, use representative chemical reactions and neglect elementary reactions. For instance, in the combustion of H_2 with O_2, the following global reaction describes two moles of hydrogen molecules reacting with one mole of oxygen to form one mole of water.

$$2H_2 + O_2 \rightarrow 2H_2O \quad (1)$$

Sequential processes with many elementary reactions that occur at the micro-kinetic level, such as equations (2)-(5), are not taken into account in equation (1) [9].

$$H_2 + O_2 \rightarrow HO_2 + H \quad (2)$$

$$H + O_2 \rightarrow HO + O \quad (3)$$

$$OH + H_2 \rightarrow H_2O + H \quad (4)$$

$$H + O_2 \rightarrow H_2O \quad (5)$$

Global kinetic models provide a general understanding of the overall chemical reactions. The classic Voltz global kinetics models describe oxidation of CO and C_3H_6 on a platinum catalyst [10]:

$$CO + \frac{1}{2}O_2 \rightarrow CO_2 \quad (6)$$

$$C_nH_m + \frac{4n+m}{4}O_2 \rightarrow nCO_2 + \frac{m}{2}H_2O \quad (7)$$

Voltz et al. developed rate equations based on a Langmuir-Hinshelwood dual-site mechanism in which two reactants that adsorb onto adjacent catalytic sites are able to react with each other [10]. A resistance term was incorporated in the rate expressions, which takes into account the inhibition effects due to chemisorption of CO and C_3H_6, the decrease of adsorbed O_2 adjacent to adsorbed CO and C_3H_6, and the inhibition effect of NO on CO and C_3H_6 oxidation rates [10]. Voltz et al. predicted CO and C_3H_6 conversions based on their rate models that satisfactorily fit their experimental data, as shown in Figure 1.3. Global kinetic models developed by Voltz et al. provide a basis for chemical kinetics modeling of catalytic aerogels.

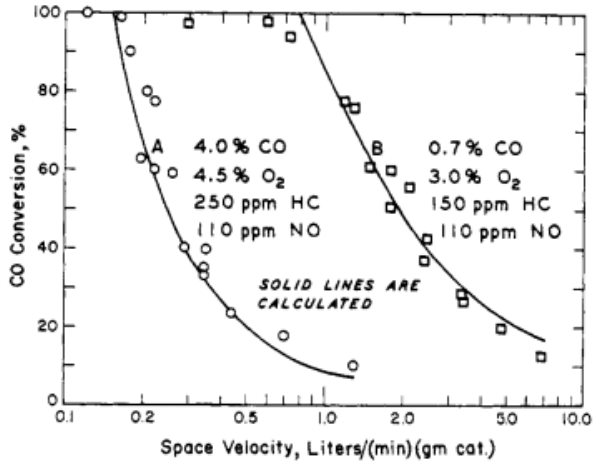

Figure 1.3. Comparison of Voltz et al. calculated (solid lines) and experimental (points) CO conversion at 288 ºC [10].

1.4 Catalytically Active Aerogels

Aerogels are a class of solid material with extremely low density, comprised of approximately 90-99% air by volume. Aerogels have a porous structure, which results in unique properties, such as high surface area, that are desired for catalysis. Union College uses a Rapid Supercritical Extraction (RSCE) technique to produce aerogels [11]. The

general process involves mixing the aerogel precursor chemicals and allowing a wet gel to form in a metal mold. The mold is placed between the platens of a hot press, which seals the wet gels in the mold and then heats the gel to achieve temperature and pressure conditions at which the solvent in the pores of the gel is in the supercritical state. The hot press restraining force is then lowered, the solvent is released as a supercritical fluid, and an aerogel is formed.

Aerogels have many applications, including use as thermal insulators, comet dust collectors, and chemical absorbers [12]. In addition, they can be very thermally stable: silica/alumina aerogels maintain thermal stability at temperatures as high as 1300 ºC, which is at the high end of the exhaust temperature range for combustion engines [13]. All these characteristics make aerogels attractive for catalytic applications in the after-treatment of automotive exhaust [4]. Catalytically active aerogels, such as cobalt-alumina aerogels, can catalyze the same reactions of converting HC, CO and NO_x to H_2O, CO_2, N_2 and O_2 [4]. Considering the cost and availability of heavy metals needed in a typical catalytic converter, catalytic aerogels are attractive as an alternative substrate coating.

Catalytic testing of aerogels has been performed on the Union College catalytic testbed (UCAT) testbed in the Union College Aerogel Lab, which simulate the conditions experienced by a conventional three-way catalyst [13]-[16]. The temperature of the gas flow can vary between 100 and 800 ºC and samples are generally tested at a space velocity of 20 s^{-1}. Space velocity is inversely proportional to the residence time of the gaseous species in the catalyst chamber: a larger space velocity corresponds to more time for the exhaust gases to react on the catalyst surface, and should thus lead to a higher percent conversion of exhaust species. Percent conversion is the percent of reactants that were

successfully converted to products, and a more efficient catalyst gives higher percent conversion values. Initial results were obtained from the UCAT-1 testbed. Figure 1.4 shows the percent conversion of HC, CO, and NO as a function of temperature for a cobalt-alumina (Co-Al) aerogel sample under stoichiometric conditions for exhaust gas containing 200 ppm C_3H_8, 300 ppm NO, 0.50 % CO and 6.05 % CO_2 (balance N_2). These results show that at high temperatures, Co-Al aerogels achieve high percent conversion of NO, HC and CO gases, and demonstrate potential as three-way catalysts.

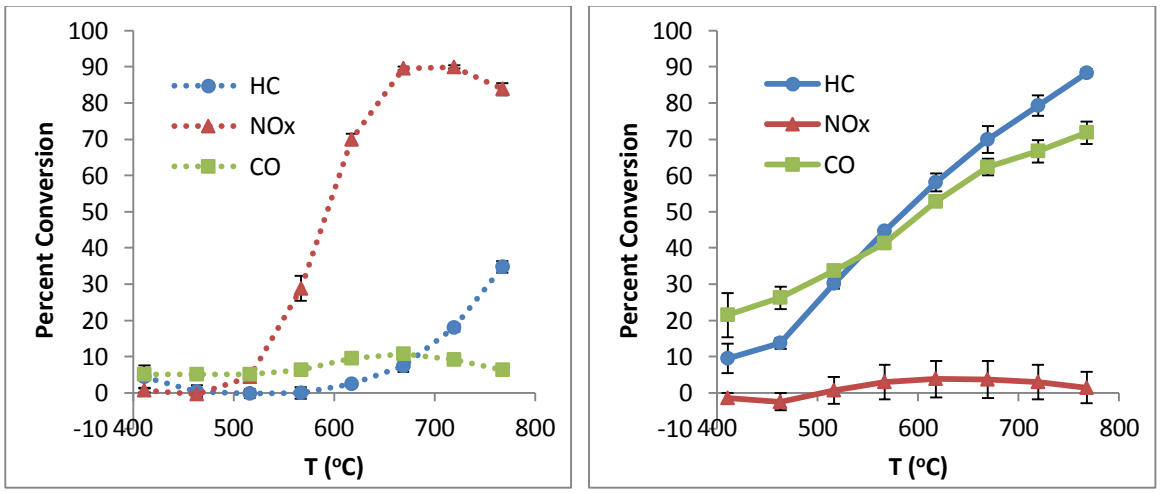

(a) (b)

Figure 1.4. Catalytic test results for a Co-Al aerogel collected at a space velocity of 20 s^{-1} for (a) pure exhaust gas, and (b) exhaust gas mixed with air at a volumetric ratio of 1:0.017 (collected by Isaac Ramphal).

1.5. Chemical Kinetics Modeling of Catalytically Active Aerogels

The study of surface catalytic reactions can contribute to a better understanding of experimental results of different types of catalytically active aerogels such as Co-Al, Cu-Al and V-Al aerogels. In this work, MATLAB is used to construct global models for the reactions to aid in understanding the reaction mechanisms and reaction rates. Initial

calculations are performed based on global model schemes for CO and propylene oxidation on platinum as carried out by Voltz et al. These models are then adjusted to simulate catalytic reactions on Co, V, and Cu species that are incorporated into the backbone of aerogel matrices.

Once these surface reactions are treated using a set of global models specific to transition metal catalysts such as vanadium, cobalt and copper, the amount of conversion products expected for reactions on catalytically active aerogels can be predicted. Kinetics parameters in these theoretical models are optimized to match with the experimental results. Optimized kinetic models aim to describe kinetic aspects of catalytic reactions and will be used to predict catalytic results for new aerogel materials.

In the following section of this thesis, I detail the fabrication and catalytic testing of Co-Al catalytic aerogels. Then the reconstruction of Voltz global kinetic model in MATLAB is described, and the results generated by this model are presented and discussed. This model was then applied to experimental data for Co-Al aerogels, and a genetic algorithm based optimization technique was used to generate values for kinetic parameters that provide the best fit to this data.

2. Catalytic Aerogel Fabrication and Properties

2.1 Aerogel Fabrication

Co-Al aerogels (~3 wt% cobalt) were fabricated for catalytic tests using the following procedure [15]. First, 2.916 g of $AlCl_3 \cdot 6H_2O$ (Fluka analytical, 99%) were dissolved in 20 mL of reagent-grade ethanol, then 9.5 mL of propylene oxide (Sigma Aldrich, reagent plus 99%) was added to the solution. A stir bar was used to stir the solution until it formed a gel. After 7 hours the gel was broken into approximately eight small pieces of similar size with a spatula. Excess solvent in the gel was decanted and replaced with a solution of 0.1146 g of $Co(NO_3)_2 \cdot 6H_2O$ (Sigma Aldrich, reagent grade 98%) in 20 mL of absolute ethanol. After another 7 hours, the excess solvent in the mixture was decanted and replaced with 20 mL of absolute ethanol. The solvent exchange with absolute ethanol was repeated once more, and the excess solvent was decanted after 7 hours. The gels were placed into a four-well mold and fresh absolute ethanol was added to fill the mold volume. This mold has a length of 12.6 cm, width of 12.6 cm, and height of 1.8 cm. Each well has a diameter of 4 cm and is 1.5 cm deep. Finally, the mold was placed into a hydraulic hot press and the gels were dried under supercritical conditions. The hot press program for fabrication of Co-Al aerogels is shown in Table 2.1.

Table 2.1. Hot press program for Co-Al aerogels.

Step	Temperature	Temperature Rate	Force	Force Rate	Dwell Time
1	32 ºC (90 ºF)	260 ºC/min (500 ºF/min)	200 kN (45 kips)	2669 kN/min (600 kip/min)	1 min
2	249 ºC (480 ºF)	2 ºC/min (4 ºF/min)	200 kN (45 kips)	4.4 kN/min (1 kip/min)	30 min
3	249 ºC (480 ºF)	93 ºC/min (200 ºF/min)	4.4 kN (1 kips)	4.4 kN/min (1 kip/min)	15 min
4	38 ºC (100 ºF)	2 ºC/min (4 ºF/min)	4.4 kN (1 kips)	2669 kN/min (600 kip/min)	1 min
5	OFF				

2.2 Properties

The supercritically processed Co-Al aerogels have a light blue color, as shown in Figure 2.1. The bulk density of similar Co-Al aerogels has been reported to be 0.051 ± 0.006 g/cm^3, with a surface area of 730 ± 20 m^2/g [15].

Figure 2.1. Photograph of Co-Al fabricated following the procedure outlined in Table 2.1.

2.3 UCAT Experimental Testing

The UCAT testbed experimentally measures the concentration of CO, NO, CO_2, O_2 and C_3H_8 through an EMS Model 5002 5-gas analyzer. Catalytic data in this work were based on two types of experiments.

The first type of experiment involves testing Co-Al aerogel at a fixed space velocity of 20 s^{-1} and a full test section (20 mL volume). The initial concentration of the species are summarized in Table 2.2. The values for CO, HC and NO are based on the gas analyzer readings of a carefully mixed tank of exhaust bland. The value for $[O_2]_o$ was found by diluting the 20.9 % of O_2 in air to the volume of gas when exhaust blend and air are mixed at a 0.017:1 ratio. During the experiment, the temperature of the test section was increased from 400 to 750 ºC. This test was performed on two aerogel samples: YC Co-Al-1 and SK_4_10, which are both Co-Al aerogels with 3 wt% cobalt.

In the second type of test, which was only performed on the SK_4_10 Co-Al aerogel, the same exhaust gas concentration and amount of aerogel catalyst were used and the testbed temperature was maintained at 600 ºC. The space velocity was increased from 14.5 to 37.0 s^{-1}. The catalytic testing results for these tests are shown in Appendices A and B.

Table 2.2. Initial concentrations of CO, O_2, HC and NO for catalytic testing of a Co-Al aerogel.

$[CO]_o$ (%)	$[O_2]_o$ (%)	$[HC]_o$ (ppm)	$[NO]_o$ (ppm)
0.5	0.354	198	300

3. Kinetic Modeling

3.1 Voltz Model

MATLAB was used to reproduce the kinetic models developed by Voltz et al. These models describe the oxidation of CO and propylene (C_3H_6) on the platinum catalyst surface (reactions (6) and (7)) and assume reaction mechanisms in which the surface reactions of chemisorbed CO and C_3H_6 with chemisorbed O_2 were the rate-determining steps (dual-site mechanism). Rate equations for CO and HC along with their corresponding rate coefficients were based on the Voltz et al. model

$$r_{CO} = -k_{r1}[CO][O_2]/R(\theta) \tag{8}$$

$$r_{C_3H_6} = -k_{r2}[C_3H_6][O_2]/R(\theta) \tag{9}$$

where k_{r1} and k_{r2} are intrinsic rate constants, [chemical formula] denotes concentration of reactant species and R(θ) is a resistance term describing the inhibitory effects on these oxidation reactions due to chemisorption of CO, NO, and C_3H_6 into the catalyst active sites,

$$R(\theta) = \{1 + k_{a1}[CO] + k_{a2}[C_3H_6]\}^2 \times \{1 + k_{a3}([CO][C_3H_6])^2\} \times \{1 + k_{a4}[NO]^{0.7}\} \tag{10}$$

where k_{a1} is the adsorption constant for CO, k_{a2} is the adsorption constant for C_3H_6, k_{a3} is the adsorption constant for the combined effect of CO and C_3H_6, and k_{a4} is the adsorption constant for NO.

The kinetic parameters k_{rj} and k_{ai} are temperature dependent and are expressed by the Arrhenius equations

$$k_{rj} = k_{rj}^0 \exp\left[-\frac{E_{ri}/R_g}{T_s+460}\right] \tag{11}$$

$$k_{ai} = k_{ai}^{0} \exp\left[-\frac{E_{ai}/R_g}{T_s+460}\right] \quad (12)$$

with j=1 for CO and j=2 for C_3H_6, and i = 1, 2, 3, and 4 as described in Equation (10). k_{rj}^{0} is the frequency factor for rate constant k_r, and k_{ai}^{0} is the frequency factor for adsorption constant k_{ai}. The frequency factor is a constant that takes into account the number of molecular collisions that have the correct orientation to generate products. E_{ri} is the activation energy for k_{rj} and E_{ai} is the activation energy for k_{ai}. R_g is the ideal gas constant (1.987 Btu/lb mol), and T_s is the catalyst temperature in ^{o}F. The values of kinetic parameters developed by Voltz et al. based on the platinum-alumina catalyst (6-8 mesh alumina spheres impregnated with platinum) are summarized in Table 3.1. The reaction temperature was 550 ^{o}F and the two initial conditions used to compare Voltz experimental results with our MATLAB adaptation of Voltz kinetic model are shown in Table 3.2.

Table 3.1. Kinetic parameters in Voltz model [10].

Parameter	Value	Parameter	Value
k_{r1}^{0}	1.83×10^{12}	E_{r1}/R_g	22600
k_{r2}^{0}	3.80×10^{13}	E_{r2}/R_g	26200
k_{a1}^{0}	6.55×10^{-1}	E_{a1}/R_g	-1730
k_{a2}^{0}	2.08×10^{-3}	E_{a2}/R_g	-650
k_{a3}^{0}	3.98×10^{-16}	E_{a3}/R_g	-20900
k_{a4}^{0}	3.02×10^{1}	E_{a4}/R_g	6720

Table 3.2. Initial conditions for testing the Voltz model: concentrations of CO, O_2, C_3H_6 and NO.

Conditions	$[CO]_o$ (%)	$[O_2]_o$ (%)	$[C_3H_6]_o$ (ppm)	$[NO]_o$ (ppm)
1	4.0	4.5	250	110
2	0.7	3.0	150	110

In the oxidation reactions of CO and C_3H_6 with O_2, the instantaneous O_2 concentration can be adjusted based on the reaction rate of CO and the stoichiometric relationship

$$2CO_{(g)} + O_{2(g)} \rightarrow 2CO_{2(g)} \tag{13}$$

The oxidation reaction of C_3H_6 is assumed to have a negligible contribution to instantaneous O_2 concentration due to the small concentration of C_3H_6, and is therefore omitted from the calculation.

A MATLAB script (Appendix C) was developed to calculate percent conversion of CO and HC as a function of space velocity. In this code, the kinetic parameters in Table 3.1, the catalyst temperature (550 ºF) and the initial gas concentrations under the two conditions listed in Table 3.2 are specified. Instantaneous concentrations of CO, HC, and O_2 are calculated every 10^{-4} s until the concentration of HC or CO reaches zero. Percent conversion of CO and HC can then be calculated based on the instantaneous and initial concentrations of CO and HC.

It is not clear from [10] how Voltz et al. calculated space velocity. In this work, reaction time *t* is used along with the reaction rate to calculate the instantaneous concentrations of reactants. Space velocity is calculated from the bulk density of the catalyst (ρ_B = 0.72 g/cm^3 for the platinum catalyst used by Voltz) and overall reaction time, as

$$\text{Space velocity}\left(\frac{L}{min\ g\ catalyst}\right) = \frac{1}{\rho_B}\left(\frac{cm^3}{g}\right) \times \frac{1\ L}{1000\ cm^3} \times \frac{1}{t\ (s)} \times \frac{60s}{1\ min} \tag{14}$$

Figures 3.1 and 3.2 compare the experimentally measured percent conversion values from Voltz et al. with the results from the MATLAB kinetics model. Figure 3.1

shows percent conversion of CO and HC as a function of space velocity when oxygen concentration is assumed to be constant throughout the reaction. Figure 3.2 shows percent conversion of these species when changes in oxygen concentration are taken into account (using the reaction in equation 13) in the rate expressions. It is not clear whether Voltz et al. took into account the changing oxygen concentration, as the resulting plots from both scenarios are similar in appearance.

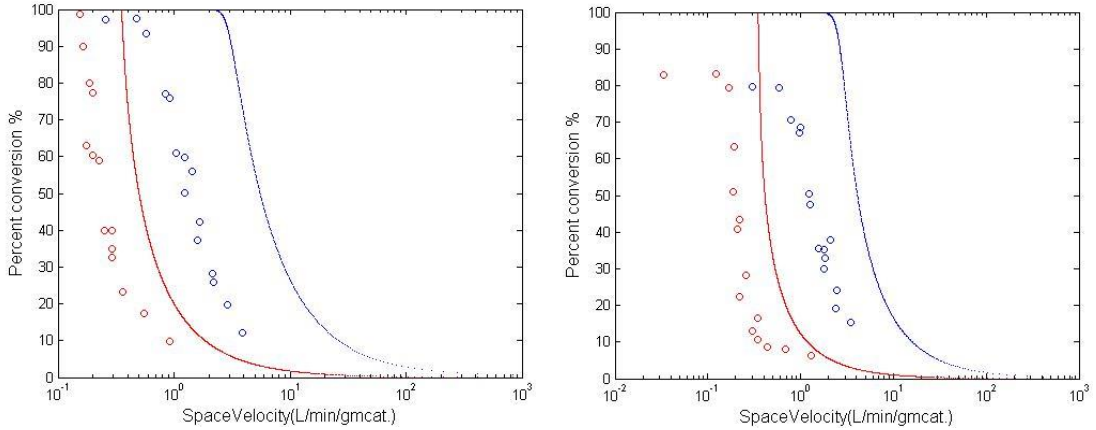

(a) (b)

Figure 3.1. Kinetic model of (a) CO and (b) HC under conditions 1 (red, data on left) and 2 (blue, data on right) with constant O_2 concentration. Solid lines are values calculated in this work and open circles are experimental data from [10].

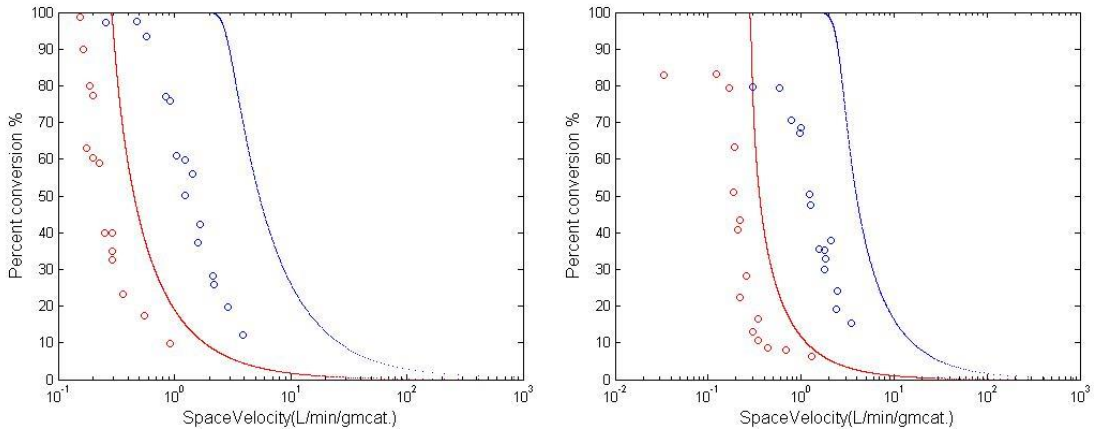

(a) (b)

Figure 3.2. Kinetics model of (a) CO and (b) HC under conditions 1 (red, data on left) and 2 (blue, data on right) with variable O_2 concentration. Solid lines are values calculated in this work and open circles are experimental data from [10].

The experimental results presented by Voltz do not agree perfectly with those of the kinetic model. Voltz model uses propylene (a C_3 species), but the Flame Ionization Detector (FID) used to measure the concentration of HCs records the concentration of C_6 species. It is unclear whether the initial concentrations of HC given by Voltz are adjusted to reflect this measurement or not. If not, then the initial amount of HC used in the Voltz model should be twice the actual concentration used experimentally. When the initial concentration was doubled, the resulting plot (Figure 3.3) shows a better match between experimental and theoretical conversion values for both CO and HC under Condition 1. Improvements in the fit between the experimental and predicted data can be seen by comparing the difference in space velocity before and after doubling HC concentration: before this, CO conversion was horizontally offset by 3.5 L/min g, whereas after the horizontal offset decreased to 2.5 L/min g. Likewise, for HC the conversion was horizontally offset 3.0 L/min g before doubling HC concentration, whereas after the horizontal offset decreased to 2.0 L/min g.

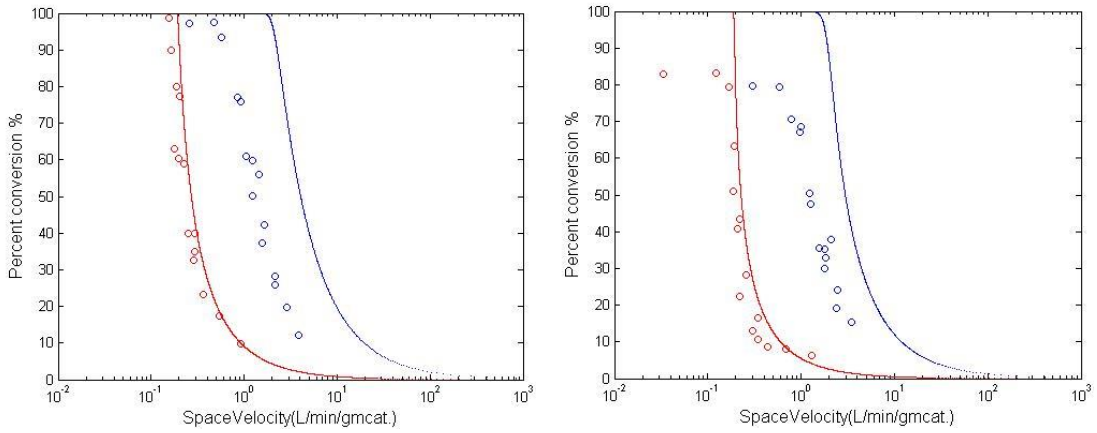

(a) (b)

Figure 3.3. Kinetics model of (a) CO and (b) HC under conditions 1 (red, data on left) and 2 (blue, data on right) with variable O_2 concentration except that concentration of HC was doubled in both cases. The solid lines are values calculated in this work and the open circles are experimental data from [10].

The Voltz kinetic model of CO and HC oxidation on a platinum catalyst was reproduced in MATLAB. Percent conversion of HC and CO were calculated as a function of space velocity, and matched reasonably well with Voltz experimental data, especially under Condition 1. These data confirm that Voltz model produces good agreement with experimental data from Voltz et al., and that this model can be implemented in MATLAB to rapidly generate predicted data for a wide variety of initial conditions and space velocities.

3.2 Application of Voltz Model to Co-Al Catalytic Test Results

The Voltz model was used to predict percent conversion of CO and HC in the UCAT testbed with a space velocity of 20 s^{-1}. UCAT investigates the conversion of CO, C_3H_8 and NO on catalytic aerogel surfaces while Voltz models conversion of CO and C_3H_6 on platinum surfaces. Since C_3H_8 is more difficult to oxidize than C_3H_6, predicting percent conversion values for our catalytic tests requires adjustment of the 'fast' HC kinetic

parameters in Table 3.1 to the 'slow' kinetic parameters given in [10]. The kinetic parameters for 'slow' HC conversion are k_{a2}^{0} = 2.0 x 10^{9} (mole %)$^{-1}$ and E_{r2}/R_g = 34,200 lb mol/Btu, respectively [10]. These values were obtained by Voltz et al. in their efforts to split the exhaust hydrocarbons into easy- and difficult-to-oxidize groups of hydrocarbons to model real engine exhaust.

The values of all other kinetic parameters for platinum in Table 3.1 were maintained when applying Voltz model to the Co-Al aerogel test data despite the fact that the catalyst employed in the experiment was a Co-Al aerogel, not platinum. As a result, the Voltz model predicted CO and HC conversions were not expected to match the UCAT experimental results. The differences between the predicted and experimental conversion values were useful in optimization steps to generate a set of kinetic parameters suitable to Co-Al aerogel catalysts.

A MATLAB script was developed to apply the Voltz model to the Co-Al aerogel test data, as shown in Appendix D. In this code, a temperature range (275 – 800 ºC) is specified and at each temperature, instantaneous concentrations of CO and HC are calculated every 10^{-7} s until the overall reaction time reaches 0.05 seconds (corresponding to a space velocity of 20 s^{-1}). Percent conversions of CO and HC at each temperature are then calculated and plotted as a function of temperature. Experimental data can also be included in the final MATLAB plot for comparison.

A comparison of the predicted HC and CO conversions at temperatures ranging from 275-800 ºC with experimentally determined HC and CO conversion at temperatures ranging from 400-800 ºC (in roughly 50 ºC increments) is shown in Figure 3.4. Changes

in oxygen concentration are taken into account in the rate expressions when calculating percent conversions.

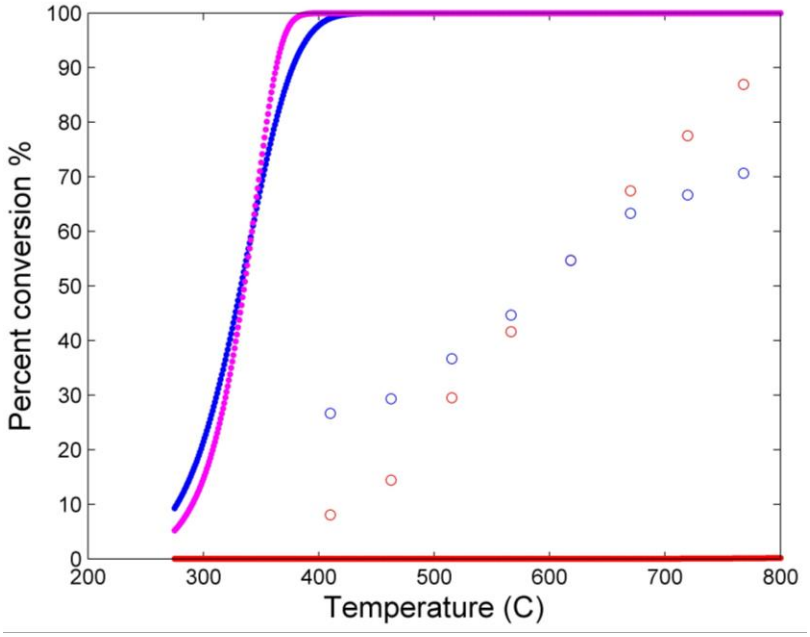

Figure 3.4. Kinetic model of CO and C_3H_8. Open circles are experimental data from the UCAT test with CY Co-Al aerogels for CO (blue) and HC (red). Filled circles are predicted CO oxidation (blue), slow HC oxidation (red) and fast HC oxidation (magenta).

As shown in Figure 3.4, the predicted CO and HC conversions do not agree with experimental data. The predicted percent conversion of CO shows a steep increase to 100% at around 400 ^{o}C, where it remains for the rest of the temperature range. The experimental data for CO conversion show a sigmoidal dependence on temperature, rising gradually from 27% at 410 ^{o}C to 71% at 770 ^{o}C. The predicted fast HC percent conversion follows a similar trend to the CO prediction. For slow HC, the percent conversion remains zero at all temperatures studied. On the other hand, the experimental HC conversion data shows an almost linear increase from 8% at 410 ^{o}C to 87% at 770 ^{o}C. The disagreement between

predicted and experimental results is assumed to result from the difference in catalyst, where experimental Co-Al results are compared to predictions from a model developed for a Pt catalyst.

4. Optimization

4.1 Manual Adjustment

Initial attempts were made to optimize the kinetic parameters developed by Voltz et al. in order to match the kinetic model with the experimental results for catalytic Co-Al aerogels. The k_a and E_r/R_g terms were held constant while the k_{r1} and k_{r2} values were varied systematically to find the minimum absolute error.

A MATLAB script was developed for optimization (Appendix E). This code searches a range of possible values for one of the kinetic parameters. At each potential value of a given kinetic parameter, percent conversion of HC and CO are calculated at each temperature of interest and compared with experimental results. The differences between predicted and experimental conversion results are summed and the value of the kinetic parameter that gives the minimum total error is determined.

The kinetic model for Co-Al aerogels after initial optimization yielded percent conversion predictions for HC and CO (Figure 4.1). Values for the original and new kinetic parameters are summarized in Table 4.1.

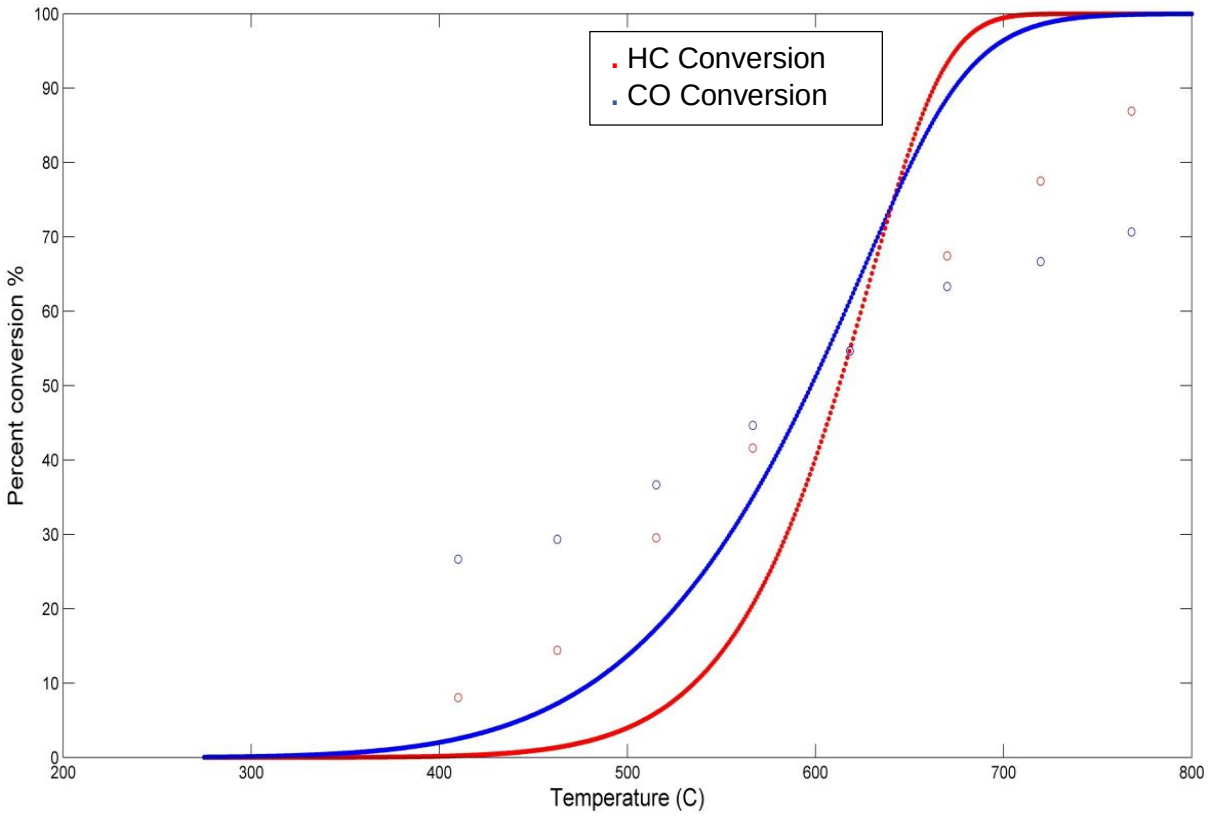

Figure 4.1. Kinetic model of CO and C_3H_8 after initial optimization. Solid lines are calculated values and open circles are experimental data from UCAT test with CY Co-Al aerogel.

Table 4.1. Summary of original [10] and new kinetic parameters after optimization.

Parameters	New Values	Original Values
k_{r1}^0	8.41×10^9	1.83×10^{12}
k_{r2}^0	1.16×10^{13}	3.80×10^{13}

To visualize the errors after optimization, MATLAB was used to plot the absolute error between predicted percentage conversion and the experimental results at each temperature tested, as shown in Figure 4.2. It is worth noticing that the error at ~620 °C

approaches zero while the rest of the errors have magnitude between 5 and 25 % conversion.

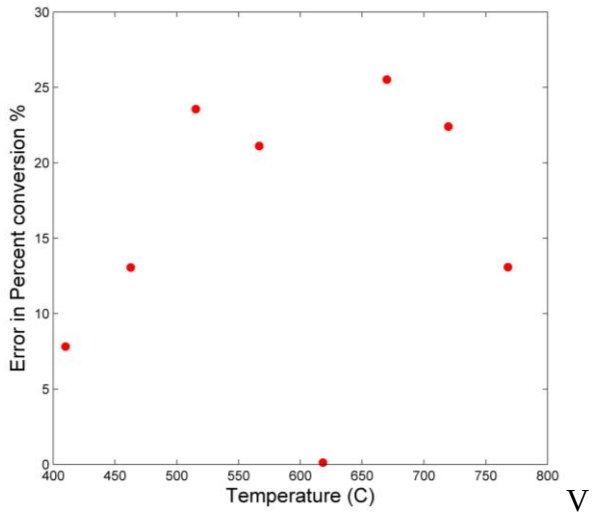

V

Figure 4.2. Absolute error in predicted and measured percent conversion for CO after initial optimization. Absolute errors are plotted at each temperature tested.

4.2 Genetic Algorithm

4.2.1 Background

Genetic algorithms (GAs), first developed by Holland in the 1960s [17], are a method that can be used for the modeling of experimental data. In this method, concepts related to natural selection are applied to data sets. A solution to a problem is described as a set of 'chromosomes' and the model fits data based on genetics-inspired operators of crossover, mutation and inversion. Chromosomes in a population, usually referring to a candidate solution to a problem, are chosen by the selection operator and the more fit chromosomes produce more offspring than the less fit ones. Two types of transformation, crossover and mutation, are used to create new offspring. The crossover operator

exchanges subparts of two chromosomes, combining parts of two individuals, which mimics biological recombination between two single-chromosome organisms. On the other hand, the mutation operator randomly changes the values present in some locations in a single chromosome. The inversion operator reverses the order of a contiguous section of the chromosome, and hence changes the order in which the genes are arrayed [17]. In this way, the GA processes populations of chromosomes and replaces one population with another. A fitness score is usually assigned to each chromosome in a given population, indicating how well the chromosome solves the problem. GA is well suited for computational problems that involve searching through a very large number of possibilities for solutions. GA enables exploring various possibilities simultaneously and offers an intelligent strategy for choosing the next set of sequences for evaluation [17].

A simple genetic algorithm works by first randomly generating a population of candidate solutions to a problem (chromosomes) and the fitness score of each chromosome in the population is calculated. Next, a pair of parent chromosomes is selected from the current population. The higher the fitness score of the chromosomes, the more likely they are to be selected, and the same chromosome can be selected more than once as a parent. Depending on the crossover probability, the pair is either crossed over to form two unique offspring or, if no crossover happens, the two offspring formed are exact copies of their parents. Depending on the mutation probability, the two offspring may be mutated and placed in the new population. Afterwards, the fitness scores of each chromosome in the new population are calculated and the selection, crossover and mutation steps are repeated until the desired number of offspring is generated [17]. Each iteration of the process produces a generation (GA typically produces 50-500 generations) and an entire set of

generations is called a run. At the end of each run, there is at least one highly 'fit' chromosome that provides a solution to the original problem [17].

4.2.2 Optimization Setup

The GA code (MCGA_20150401_SIMPLE) used in this work is based on unpublished work [18]. Two input files (a MATLAB script and an excel file) are required to use the code. The script, *feasymodel.mat,* specifies kinetic parameters, simulation time, initial conditions and differential equations. The excel spreadsheet, *sheeteasychem1.xls,* contains possible ranges for ach parameter, optimization parameters and experimental data.

Three differential equations, dy(1)/dt, dy(2)/dt and dy(3)/dt, were used to describe reactions (8), (9) and (13), which correspond to the reaction rates of CO, HC and O_2, in the feasymodel script. These differential equations were based on (8), (9), (10) and (13), except that the negative signs in front of E_3R_3, E_4R_4 and E_5R_5 (corresponding to E_{a1}/R_g, E_{a2}/R_g and E_{a3}/R_g in Table 3.1) were omitted and the E_3R_3, E_4R_4 *and* E_5R_5 terms in the differential equations were given the opposite sign as the original value. This is to ensure that all the kinetic parameters in the differential equations have positive values, which simplifies the optimization boundary setting. The variable NO was substituted with the actual concentration of the species (110 ppm) assuming that NO concentration stays constant. Concentrations of CO, HC and O_2 were represented as y(1), y(2) and y(3), respectively, in the differential equations shown in Appendix F.

4.2.3 Voltz Optimization

To test whether GA is a viable method for optimizing the kinetic model and finding optimal kinetic parameters, the GA code was used to search values for all of the kinetic parameters in Table 3.1 that fit the Voltz et al. experimental data best. Experimental data used for this fitting purpose were taken from percent conversion results for CO and C_3H_6 on a platinum catalyst at 288 ºC (550 ºF) from Figures 21 and 22 in Voltz et al. [10]. Space velocities were converted to reaction time based on equation 14, and instantaneous concentrations of CO and HC were calculated based on their initial concentrations and their percent conversion results at each space velocity [10]. The corresponding script and spreadsheet are shown in Appendices G and H.

The optimal kinetic parameters obtained through GA are summarized in Table 4.2 and compared to the original kinetic parameters given in Voltz et al. These optimized parameters were used in the Voltz model to generate predicted data of percent conversion as a function of space velocity. These predicted data were compared to Voltz experimental data, and were found to fit well, as shown in Figure 4.3.

Table 4.2. Summary of original and optimized kinetic parameters through GA.

Parameters	Voltz Values [10]	Optimized Values	Parameters	Voltz Values	Optimized Values
k_{r1}^0	1.83×10^{12}	1.67×10^{12}	E_{r1}/R_g	22600	24377
k_{r2}^0	3.80×10^{13}	3.85×10^{13}	E_{r2}/R_g	26200	27888
k_{a1}^0	6.55×10^{-1}	4.11×10^{-1}	E_{a1}/R_g	-1730	-1696
k_{a2}^0	2.08×10^{-3}	1.11×10^{-3}	E_{a2}/R_g	-650	-469.8
k_{a3}^0	3.98×10^{-16}	4.05×10^{-16}	E_{a3}/R_g	-20900	-19102
k_{a4}^0	3.02×10^{1}	2.50×10^{1}	E_{a4}/R_g	6720	6514

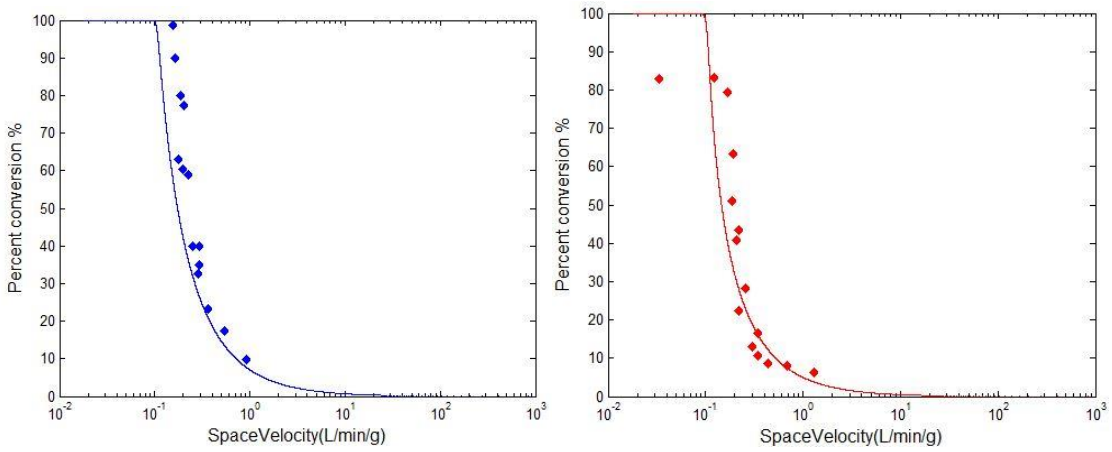

(a) (b)

Figure 4.3. Kinetic model of (a) CO and (b) HC with GA optimized kinetic parameters. The solid lines are values calculated in this work and the points are experimental data from Voltz et al.

A comparison of the predicted data in Figure 4.3 with those in Figure 3.3, where Voltz original kinetic parameters were used, shows that the GA optimization produces a similar agreement with Voltz experimental data. As shown in Table 4.2, the GA optimized and Voltz original values differ only slightly from one another. The GA optimized values for k_{r2}^0, k_{a3}^0, E_{r2}, E_{a1} , E_{a2}, E_{a3} are larger than Voltz original values and the rest of the parameters are smaller than his parameters. It is difficult to tell whether the GA optimized or Voltz original kinetic parameters produce a better fit to Voltz experimental data, and therefore better values for the kinetic model. The original values were obtained by Voltz et al. several decades ago and it is possible that by using the more advanced GA optimization technique we have found better kinetic parameters to fit Voltz model.

4.2.4 UCAT Optimization

GA was then used to obtain kinetic parameters based on UCAT Co-Al aerogel data. Varying space velocity catalytic data at 600 ºC from SK 4_10 Co-Al aerogel in Appendix B were used as experiment data and the corresponding optimization script and spreadsheet are shown in Appendices J and K. The GA fitting to these experimental data is shown Figure 4.4. The optimized kinetic parameters are summarized in Table 4.3. These parameters were then used in the kinetic model to predict % conversion for HC and CO across a large temperature range and compared to experimental results for SK 4_10 Co-Al aerogel, as shown in Figure 4.5.

Table 4.3. Summary of original Voltz kinetic parameters and optimized parameters for Co-Al aerogels.

Parameters	**Voltz Values** (*10*)	**Optimized Values**	**Parameters**	**Voltz Values**	**Optimized Values**
k_{r1}^0	1.83×10^{12}	1.09×10^{6}	E_{r1}/R_g	22600	529.90
k_{r2}^0	3.80×10^{13}	4.83×10^{6}	E_{r2}/R_g	26200	2717.5
k_{a1}^0	6.55×10^{-1}	5.65×10^{-7}	E_{a1}/R_g	-1730	-229.3
k_{a2}^0	2.08×10^{-3}	1.34×10^{-6}	E_{a2}/R_g	-650	-5.14
k_{a3}^0	3.98×10^{-16}	4.70×10^{-19}	E_{a3}/R_g	-20900	-26810
k_{a4}^0	3.02×10^{1}	2.84×10^{2}	E_{a4}/R_g	6720	19.89

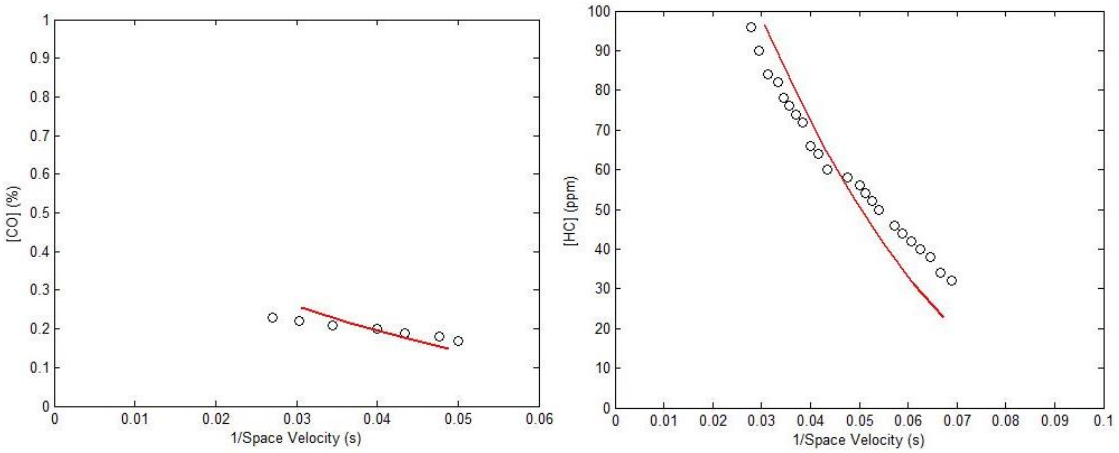

(a) (b)

Figure 4.4. The GA fitting to the SK 4_10 Co-Al aerogel experimental (a) CO and (b) C_3H_8 at 600 ºC and various space velocity.

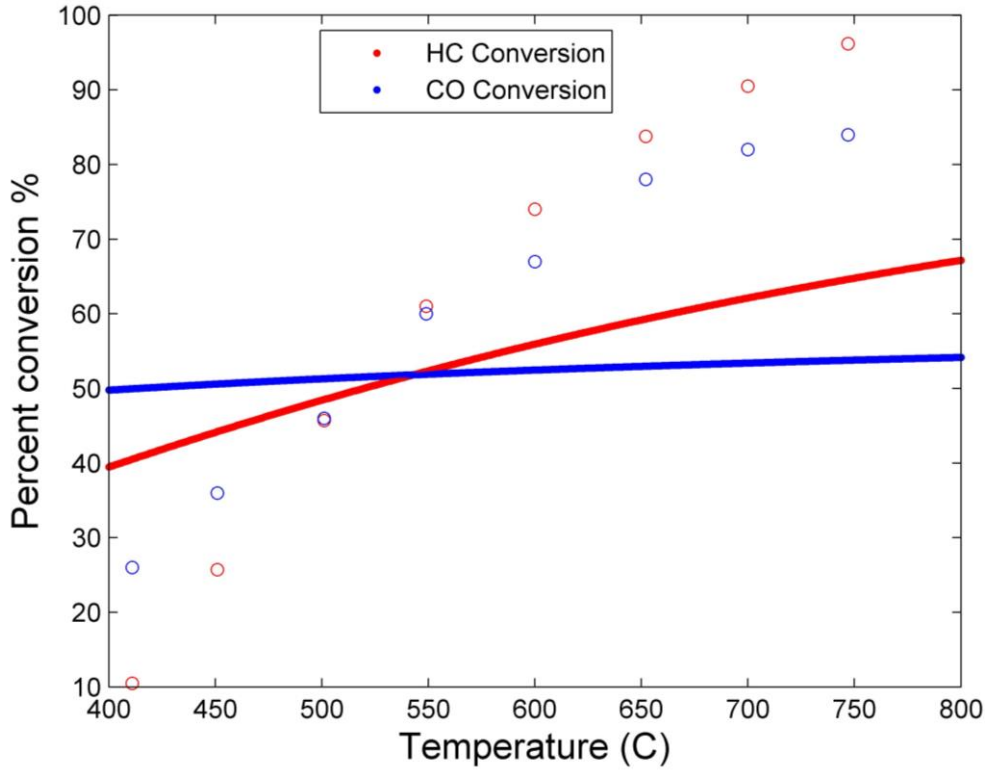

Figure 4.5. Kinetic model of CO and C_3H_8 after GA optimization. Solid lines are calculated values and open circles are experimental data from UCAT test with SK_4_10 Co-Al aerogel.

As shown in Figure 4.4, at 600 ºC, the GA fitting to the experimental SK_4_10 Co-Al aerogel data at various space velocity is reasonably good. Figure 4.5 shows that the calculated percent conversion values yield similar trends, but do not match experimental results for either HC or CO exactly across the entire temperature range. This is not especially surprising, as the kinetic parameters used to generate these calculated values across such a large temperature range from 400-800 ºC were optimized using varying space velocity data which was only available at 600 ºC. The errors between calculated and experimental conversions are smallest in the 500- 600 ºC range. At temperatures lower than 550 ºC, the predicted conversions are higher than experimental values, while at higher temperatures the experimental conversions are higher than those predicted. To obtain a better fit with the experimental results, varying space velocity data at all temperature of interest should be obtained and used to optimize kinetic parameters.

Although it is important to more accurately determine the kinetic parameters given in Table 4.3, the rate constants $k_{r1,}\, k_{r2}$ for CO and HC oxidation in equations (8) and (9) and adsorption constants $k_{a1,}\, k_{a2,}\, k_{a3}$ and k_{a4} in equation (10), can be determined at temperatures of interest from equations (11) and (12). Values of $k_{r1,}\, k_{r2,}\, k_{a1,}\, k_{a2,}\, k_{a3}$ and k_{a4} based on GA optimized parameters, which correspond to a Co-Al catalyst, and Voltz original parameters, which correspond to a Pt catalyst, are summarized in Table 4.4. These parameters are temperature dependent and were evaluated at temperatures for which the experimental Co-Al aerogel percent conversion data were collected.

Table 4.4. Rate constants and adsorption constants determined from Voltz and GA optimized kinetic parameters at various temperatures.

Temperature (ºC)		411	451	501	549	600	652	700	747
Pt Catalyst	k_{r1}	1.97×10^{4}	5.43×10^{4}	1.66×10^{5}	4.28×10^{5}	1.04×10^{6}	2.34×10^{6}	4.57×10^{6}	8.29×10^{6}
	k_{r2}	2.20×10^{4}	7.12×10^{4}	2.61×10^{5}	7.81×10^{5}	2.20×10^{6}	5.60×10^{6}	1.22×10^{7}	2.42×10^{7}
	k_{a1}	2.67	2.47	2.27	2.11	1.97	1.85	1.76	1.68
	k_{a2}	3.53×10^{-3}	3.42×10^{-3}	3.32×10^{-3}	3.23×10^{-3}	3.15×10^{-3}	3.07×10^{-3}	3.01×10^{-3}	2.96×10^{-3}
	k_{a3}	9.30×10^{-9}	3.64×10^{-9}	1.29×10^{-9}	5.40×10^{-10}	2.37×10^{-10}	1.12×10^{-10}	6.04×10^{-11}	3.48×10^{-11}
	k_{a4}	0.129	0.174	0.243	0.322	0.42	0.534	0.652	0.778
Co-Al aerogel catalyst	k_{r1}	7.07×10^{5}	7.24×10^{5}	7.44×10^{5}	7.60×10^{5}	7.76×10^{5}	7.91×10^{5}	8.04×10^{5}	8.15×10^{5}
	k_{r2}	5.32×10^{5}	6.01×10^{5}	6.88×10^{5}	7.71×10^{5}	8.58×10^{5}	9.45×10^{5}	1.02×10^{6}	1.10×10^{6}
	k_{a1}	7.20×10^{-7}	7.11×10^{-7}	7.00×10^{-7}	6.92×10^{-7}	6.83×10^{-7}	6.76×10^{-7}	6.70×10^{-7}	6.65×10^{-7}
	k_{a2}	1.35×10^{-6}	1.35×10^{-6}	1.34×10^{-6}	1.34×10^{-6}	1.34×10^{-6}	1.34×10^{-6}	1.34×10^{-6}	1.34×10^{-6}
	k_{a3}	1.33×10^{-9}	4.01×10^{-10}	1.06×10^{-10}	3.46×10^{-11}	1.20×10^{-11}	4.60×10^{-12}	2.08×10^{-12}	1.03×10^{-12}
	k_{a4}	280	280.3	280.6	280.8	281	281.2	281.4	281.5

According to Table 4.4, the rate constants for CO and HC oxidation are larger for Co-Al aerogel catalyzed reactions than for Pt catalyzed reactions at temperatures below 600 ºC. At temperatures above 600 ºC, the opposite trend is observed. In addition, according to equation (10), k_{a1} and k_{a2} are related to the inhibition effect due to chemisorption of CO and HC, k_{a3} is related to the decrease of adsorbed O_2 adjacent to adsorbed high-concentration CO and HC, and k_{a4} is related to inhibition effect of NO. The smaller k_{a1}, k_{a2} and k_{a3} values at all temperatures in the Co-Al catalyzed reactions, relative to those for Pt catalyzed reactions, indicate that CO and HC adsorb better on a Pt metal surface. Co-Al aerogels might adsorb NO better than does Pt considering that all the k_{a4} values for Co-Al aerogel catalyzed reactions are much larger than those for Pt. These preliminary comparisons and tentative conclusions about the properties of Co-Al and Pt as catalysts are based on the assumption that the kinetic parameters in Table 4.3 are accurately determined. Since it is clear that the optimized kinetic parameters do not give a very good

fit across the range of experimental conversion data collected, such a comparison requires better fitting of Figure 4.5 through GA with more UCAT experimental data if it is to be meaningful.

5. Conclusions and Future Work

A kinetic model for describing the oxidation of CO and HCs on Co-Al aerogel catalysts was developed based on Voltz global model for platinum catalysts. This model successfully predicted percent conversion results for CO and C_3H_6 that agreed well with Voltz experimental data, confirming the results of Voltz et al. When applied to UCAT Co-Al experimental data, Voltz platinum parameters produced, as anticipated, a poor fit to the percent conversion results for CO and C_3H_8. GA based optimization was performed and kinetic parameters were adjusted to better fit experimental data. A fair agreement with the experimental Co-Al aerogel over a range of temperatures was achieved after calibrating the parameters with experimental results at 600 ºC with varying space velocities. Rate constants for CO and HC oxidation reactions and adsorption constants were determined at various temperatures from GA optimized parameters, and comparison of the properties of Co-Al aerogel and Pt catalysts were made based on these preliminary results.

Future work should include further optimization of the kinetic model for Co-Al aerogels. Voltz kinetic model was based on experimental results at fixed temperature with various space velocity, and it produced good fit at this specific temperature. To further develop a comprehensive and robust kinetic model for catalytic aerogels and to make more convincing and accurate comparison of Co-Al aerogel as a catalyst, additional experimental data obtained over a larger range of space velocities at each temperature of interest must be acquired. This type of kinetic model will then be developed for other types of catalytically active aerogels such as Cu-Al, Cu-Si, Co-Si, V-Si and Ni-Al aerogels, and will be extended to describe changes in NO concentration. The kinetic parameters for each model will be determined via GA based optimization, which will enable direct quantitative

comparison of catalytic capabilities of different types of aerogels from a kinetic perspective.

References

1. Faiz, A.; Weaver, C. S.; Walsh, M. P. Air Pollution from Motor Vehicles. The International Bank: Washington, D.C., 1996; pp 2-6.

2. Deur, J. M. Simulation of Engine Exhaust Aftertreatment with CFD using detailed chemistry. *Eleventh International Engine Combustion Multi-Dimensional Modeling Conference*, 2001.

3. Brandt, E. P.; Wang, Y.; Grizzle, J. W. Dynamic Modeling of a Three-Way Catalyst for SI Engine Exhuast Emiision Control. *IEEE Transactions on Control Systems Technology* **1999,** *XX* (Y), 1-9.

4. Bruno, B. A.; Madero, J. E.; Juhl, S. J.; Rodriguez, J.; Dunn, N. J. H.; Carroll, M. K.; Anderson, A. M. Alumina-Based Aerogels as Three-Way Catalysts. *Conference proceedings of the Ninth International Congress on Catalysis and Automotive Pollution Control (CAPoC9)*, August 2012.

5. Catalytic converter. http://preciousmetals.umicore.com/recyclables/SAC/CatalyticConverter/ (accessed Nov 16, 2014).

6. Nair, N. *A Computationally Efficient Model for the Simulation of Catalytic Monolith Reactors with Detailed Chemistry;* The Ohio State University, 2013.

7. Sampara, C. S. *Global Reaction Kinetics for Oxidation and Storage in Diesel Oxiadation Catalysts;* PhD Thesis; The University Of Michigan: Ann Arbor, 2008.

8. Chatterjee, D.; Deutschmann, O.; Warnatz, J. Detailed surface reaction mechanism in a three-way catalyst. *Faraday Discuss.* **2001,** *119*, 371-384.

9. Guelder, O. L. AER 1304 Fundamentals of Combustion, 2012. Univeristy of Toronto Institute for Aerospace Studies. http://arrow.utias.utoronto.ca/~ogulder/ClassNotes2.pdf (accessed November 18, 2014).

10. Voltz, S. E.; Morgan, C. R.; Liederman, D.; Jacob, S. M. Kinetic Study of Carbon Monoxide and Propylene Oxidation on Platinum Catalysts. *Ind. Eng. Chem. Prod. Res. Develop.* **1973,** *12* (4), 294-301.

11. Gauthier, B. M.; Bakrania, S. D.; Anderson, A. M.; Carroll, M. K. A fast supercritical extraction technique for aerogel fabrication. *Journal of Non-Crystalline Solids* **2004,** *350,* 238-243.

12. Pajonl, G. M. Catalytic Aerogels. *Catalysis Today* **1997,** *35,* 319-337.

13. Rodriguez, J. *Design and Testing of the Catalytic Test Bed, and Testing of Catalytic Aerogels;* Undergraduate Thesis; Union College: New York, 2011.

14. Brockmann, P. *The Redesign of the Union Catalytic Testbed;* Senior Thesis; Union College: Schenectady, 2013.

15. Juhl, S. J. *Characterization of Alumina-Based Aerogels Made by Rapid Supercritical Extraction for Use in Automotive Catalysis.;* Summer Research Report; Union College: Shenectady, 2012.

16. Swanton, T. *Design of a Gas Conditioning System for the Second Generation Union College Aerogel Lab Catalytic Test Bed;* Senior Thesis; Union College: Schenectady, 2013.

17. Mitchell, M. *An Introduction to Genetic Algorithms;* MIT: Boston, 1996.

18. Berkemeier, T. Unpulished results from the Max Planck Institute for Chemistry, Mainz, Germany.

Appendix A. All Temperature Data of YC Co-Al-1 Aerogel and SK 4_10 (Co-Al) Aerogel.

Table A.1 Percent conversion results of YC Co-Al-1 aerogel at various temperatures with blend air.

Run #	T (°F)	HC % Conversion	CO % Conversion
1	770.0	8	27
2	864.8	14	29
3	959.6	30	37
4	1052	42	45
5	1145	55	55
6	1238	67	63
7	1327	78	67
8	1414	87	71

Table A.2 Percent conversion results of SK 4_10 Co-Al aerogel at various temperatures with blend air.

Run #	T (°F)	HC % Conversion	CO % Conversion
1	771.8	11	26
2	843.8	26	36
3	933.8	46	46
4	1020.2	61	60
5	1112	74	74
6	1205.6	84	78
7	1292	91	82
8	1376.6	96	84

Appendix B. Varying Space Velocity Data of SK 4_10 Co-Al aerogel.

Table B.1 Percent conversion results of SK 4_10 Co-Al aerogel at space velocity with blend air at 600 ºC.

Space Velocity (s^{-1})	HC % Conversion	CO % Conversion
14.5	85	65
15.0	84	63
15.5	82	63
16.0	81	65
16.5	80	65
17.0	79	65
17.5	78	65
18.0	78	65
18.5	76	65
19.0	75	67
19.5	75	67
20.0	74	67
21.0	73	65
22.0	78	63
23.0	72	63
24.0	70	62
25.0	69	62
26.0	66	62
27.0	65	62
28.0	64	62
29.0	63	60
30.0	61	60
31.0	59	60
32.0	60	58
33.0	58	58
34.0	58	56
35.0	55	56
36.0	55	56
37.0	56	56

Appendix C. MATLAB Script for Voltz Model.

```
% Recreate global model of CO and Propylene Oxidation on Platinum
Catalyst
% Paper Author: Voltz, S.E. Mobile Research and Development Corp,
N.J.1973.
% MATLAB Author: Yi Cao, caoy@union.edu
% Union College, Chemistry and Mechanical Engineering Department
% Last update: 2015/01/17
% Note: initial conditions are based on conditions listed on the left
of Fig 21 in the paper
%En(Btu/(lb mol)) stands for activation energy for krn
%All the R values are equal to ideal gas constant: 1.987 Btu/(lb mol)
%All the E and R values below came from Table I in Voltz et al.
E1_R1 = 22600;
E2_R2 = 26200;
E3_R3 = -1730;
E4_R4 = -650;
E5_R5 = -20900;
E6_R6 = 6720;
%k0rn is the frequency factor for krn
%k0an is the frequency factor for kra
%Frequency factor values below came from Table I in Voltz et al.
k0r1 = 1.83*10^(12);
k0r2 = 3.80*10^(13);
k0a1 = 6.55*10^(-1);
k0a2 = 2.08*10^(-3);
k0a3 = 3.98*10^(-16);
k0a4 = 3.02*10^(1);
%Ts is the catalyst temperature in F.
%Conditions in Figure 21 specify catalyst temperature to be 550 F
Ts = 550;
%The temperature of the kinetic parameters krn and kan are expressed in
Arrhenius equations
kr1 = k0r1 * exp(-E1_R1/(Ts+460));
kr2 = k0r2 * exp(-E2_R2/(Ts+460));
ka1 = k0a1 * exp(-E3_R3/(Ts+460));
ka2 = k0a2 * exp(-E4_R4/(Ts+460));
ka3 = k0a3 * exp(-E5_R5/(Ts+460));
ka4 = k0a4 * exp(-E6_R6/(Ts+460));
%Define initial condition as t =0
%Initial concentrations HCi, COi, NOi, and O2i are based on the
conditions listed on the left of Fig 21
%Note here NO, CH are concentration in ppm, O2, CO are in mole per cent
%Use the values with the given unit as stated in Voltz
t =0;
HCi = 250;
COi = 4;
NOi = 110;
O2i = 4.5;
%Define HC, CO, NO and O2 to be instantaneous concentrations. At t=0,
instantaneous concentration is the same as initial concentrations
HC = HCi;
CO = COi;
NO = NOi;
O2 = O2i;
%A loop is used to calculate the change in concentration of CO and HC
```

```
%Concentration changes are evaluated until the concentrations of HC and
CO drop below zero
%Time step is 0.0001
while (HC>0 & CO>10e-100)
%BigR is defined to account for inhibition effects due to chemisorption
of CO and HC
%The last term in the expression accounts for the inhibition effect of
%NO on both oxidation rates
BigR = (1+ ka1* CO + ka2*HC)^2 *(1+ka3*(CO*HC)^2)*(1+ka4*(NO)^.7);
%Rate equations: krn is rate constants and BigR includes inhibition
%effect of CO, CH and NO
rCO = - kr1 * CO* O2/BigR;
rHC = - kr2 * HC* O2/BigR;
%Instantaneous concentration of CO and HC is adjusted
CO_new = CO + rCO * 0.0001;
HC_new = HC + rHC * 0.0001;
%O2 concentration can also be adjusted using the equation below as O2
%is consumed mainly in oxidation of CO.
O2_new = O2 + 0.5*rCO*0.0001;
%Percentage conversion calculation
conversion_HC = (HCi-HC_new) / HCi *100;
conversion_CO = (COi-CO_new) / COi *100;
%Space velocity is calculated based on the bulk density of the platinum
catalyst in Voltz experiment: 0.72 g/cm^3. The space
%velocity has the unit L/min/gm_catalyst.
spaceV = 60/0.72/t/1000;
%Plot the conversion percentage as a function of time
%Semilog plot helps visually observe the data trend
%the ones with % can be used to plot conversion rate with time
semilogx(spaceV,conversion_CO,'r')
hold on
semilogx(spaceV,conversion_HC,'g')
%Assign instantaneous new value to present concentration and repeat
loop
CO=CO_new;
HC = HC_new;
O2= O2_new;
t=t+0.0001;
end
hold on
% Load voltz data file for experimental data on space velocity and CO
conversion to compare with model results
load voltzco1.txt;
SV1 = voltzco1(1:15,1)';
PCCO1 = voltzco1(1:15,2)';
scatter(SV1,PCCO1,25,'r')
hold on
% Load voltz data file for experimental data on space velocity and HC
conversion to compare with model results
load voltzhc1.txt;
SV1 = voltzhc1(1:15,1)';
PCHC1 = voltzhc1(1:15,2)';
scatter(SV1,PCHC1,25,'g')
%Label the plot
title('Kinetics Model of CO and HC with O2 Change','FontSize',15)
xlabel('SpaceVelocity(L/min/gmcat.)', 'FontSize',12)
ylabel('Percent conversion %','FontSize',12)
```

```
legend('CO Conversion', 'HC Conversion
```

Appendix D. MATLAB Script for Applying Voltz Model to UCAT Co-Al-1 Test.

```
% Recreate global model of CO and Propylene Oxidation on Platinum
Catalyst
% Paper Author: Voltz, S.E. Mobile Research and Development Corp,
N.J.1973.
% MATLAB Author: Yi Cao, caoy@union.edu
% Union College, Chemistry and Mechanical Engineering Department
% Last update: 2015/02/01
% Note: initial conditions based on UCAT CO-Al-1
%En(Btu/(lb mol)) stands for activation energy for krn
%All the R values are equal to ideal gas constant: 1.987 Btu/(lb mol)
%All the E and R values below came from Table I in Voltz et al. except
that E2_R2 was adjusted to account for propane (difficult to oxidize
hydrocarbons)
E1_R1 = 22600;
E2_R2 = 34200;
E3_R3 = -1730;
E4_R4 = -650;
E5_R5 = -20900;
E6_R6 = 6720;
%k0rn is the frequency factor for krn
%k0an is the frequency factor for kra
%Frequency factor values below came from Table I in Voltz et al. except
that E2_R2 was adjusted to account for propane (difficult to oxidize
hydrocarbons)
k0r1 = 1.83*10^(12);
%Frequency factor values below came from Table I in Voltz et al. except
that E2_R2 was adjusted to account for propane (difficult to oxidize
hydrocarbons)

k0r2 = 2.0*10^(9);
k0a1 = 6.55*10^(-1);
k0a2 = 2.08*10^(-3);
k0a3 = 3.98*10^(-16);
k0a4 = 3.02*10^(1);
%Initial concentrations HCi, COi, NOi, and O2i are average measured
concentration for UCAT Co-Al-1 test
%Note here NO,CH are concentration in ppm, O2, CO are in mole per cent
%Use the values with the given unit as stated in Voltz
HCi = 198;
COi = 0.5;
NOi = 300;
O2i = 0.354;
%Define HC, CO, NO and O2 to be instantaneous concentrations. At t=0,
instanenous concentration is the same as initial concentrations
HC = HCi;
CO = COi;
NO = NOi;
O2 = O2i;
%Assign initial value of the temperature of the catalyst at 275 oC.
Ts=275;
%Start counter at i=1 for loop below.
i=1;
%A loop is used to calculate the change in concentration of CO and HC
%Concentration changes are evaluated at t=0.05 which corresponds to the
%UCAT space velocity of 20 (s^-1) for testing
```

```
%Time step is 0.0000001
step= 0.0000001;
for Ts=275:800;
%Set the initial concentrations of reactants to original values
HC = HCi;
CO = COi;
NO = NOi;
O2 = O2i;
%The temperature of the kinetic parameters krn and kan are expressed in
Arrhenius equations
%Note here the Ts is converted to oF as oF is used in the original
 equation from Voltz.
 kr1 = k0r1 * exp(-E1_R1/((1.8*Ts+32)+460));
 kr2 = k0r2 * exp(-E2_R2/((1.8*Ts+32)+460));
 ka1 = k0a1 * exp(-E3_R3/((1.8*Ts+32)+460));
 ka2 = k0a2 * exp(-E4_R4/((1.8*Ts+32)+460));
 ka3 = k0a3 * exp(-E5_R5/((1.8*Ts+32)+460));
 ka4 = k0a4 * exp(-E6_R6/((1.8*Ts+32)+460));
 t=0;
%Space velocity tested in UCAT system is 20 s-1, which corresponds to
time 0.05 s.
while t<0.05
%BigR is defined to account for inhibition effects due to
%chemisorption of CO and HC
%The last term in the expression accounts for the inhibition effect of
%NO on both oxidation rates
 BigR = (1+ ka1* CO + ka2*HC)^2 *(1+ka3*(CO*HC)^2)*(1+ka4*(NO)^.7);
%Rate equations: krn is rate constants and BigR includes inhibition
effect of CO, CH and NO
 rCO = - kr1 * CO* O2/BigR;
 rHC = - kr2 * HC* O2/BigR;
%Instantaneous concentration of CO and HC is adjusted.
 CO_new = CO + rCO * step;
 HC_new = HC + rHC * step;
%O2 concentration can also be adjusted using the equation below as O2
is consumed mainly in oxidation of CO
 O2_new = O2 + 0.5*rCO*0.001;
%Percentage conversion calculation
 conversion_HC = (HCi-HC_new) / HCi *100;
 conversion_CO = (COi-CO_new) / COi *100;
%Assign instantaneous new value to present concentration and repeat
loop
 CO=CO_new;
 HC = HC_new;
 O2=O2_new;
 t=t+ step;
 end
%Plot the %conversion of HC and CO as a function of Ts
 plot(Ts,conversion_HC,'.r','MarkerSize',9)
 hold on
 plot(Ts,conversion_CO,'.b','MarkerSize',9)
 i=i+1;
end
 %Load UCAT data file for experimental data on temperature and HC
conversion to compare with model results
load CoAl_HC.txt;   % this is the data file for space velocity and HC
conversion
```

```
 Temp = CoAl_HC(1:8,1)';
 PCHC = CoAl_HC(1:8,2)';
 scatter(Temp,PCHC,25,'r')
 hold on
%Load UCAT data file for experimental data on temperature and CO
conversion to compare with model results
 load CoAl_CO.txt;   % this is the data file for space velocity and CO
conversion
 Temp = CoAl_CO(1:8,1)';
 PCCO = CoAl_CO(1:8,2)';
 scatter(Temp,PCCO,25,'b')
%Label the plot
 title('Kinetics Model of UCAT CO-Al-1 Test with O2
Change','FontSize',15)
 xlabel('Temperature (oC)', 'FontSize',12)
 ylabel('Percent conversion %','FontSize',12)
 legend('HC Conversion','CO Conversion')
```

Appendix E. MATLAB Script for Manual Adjustment Optimization.

```
% Optimization for Kinetic Parameters in Voltz Model
% MATLAB Author: Yi Cao, caoy@union.edu
% Union College, Chemistry and Mechanical Engineering Department
% Last update: 2015/03/08
 %En(Btu/(lb mol)) stands for activation energy for krn
 %All the R values are equal to ideal gas constant: 1.987 Btu/(lb mol)
 %All the E and R values below came from Table I in Voltz et al. and
 %assumed constant
 E1_R1 = 22600;
 E2_R2 = 34200;
 E3_R3 = -1730;
 E4_R4 = -650;
 E5_R5 = -20900;
 E6_R6 = 6720;
 %k0rn is the frequency factor for krn
 %k0an is the frequency factor for kra
 %Frequency factor values below came from Table I in Voltz et al.
 %Comment on the parameter that is subject to optimization, and in this
 %case, the k0r1
 %k0r1 = 1.83*10^(12);
 k0r2 = 3.80*10^(-1);
 k0a1 = 6.55*10^(-1);
 k0a2 = 2.08*10^(-3);
 k0a3 = 3.98*10^(-16);
 k0a4 = 3.02*10^(1);
 %Initial concentrations HCi, COi, NOi, and O2i are average measured
 %concentration for UCAT Co-Al-1 test
 %Note here NO,CH are concentration in ppm, O2, CO are in mole per cent
 %Use the values with the given unit as stated in Voltz
    HCi = 99*2;%HC measured by gas analyser is half of real amount
    COi = 0.5;
    NOi = 300;
    O2i = 0.354;
    HC = HCi;
    CO = COi;
    NO = NOi;
    O2 = O2i;
  %Start searching k values across a range
  %kr0 is the starting value
  kr0=0.8E+10;
  k0r1=0;
  step=1*10^(4);
 %Vary k values across the range below and calculate errors in percent
 %conversion
  for m=1:1000
  k0r1 = step*m+kr0;
i=1;
for Ts=[410, 462.7, 515.3, 566.7, 618.3, 670, 719.7, 768];
%Reset initial values for reactants
   HCi = 99*2;%HC measured by gas analyser is half of real amount
   COi = 0.5;
   NOi = 300;
   O2i = 0.354;
   HC = HCi;
   CO = COi;
```

```
   NO = NOi;
   O2 = O2i;
%The temperature of the kinetic parameters krn and kan are expressed in
Arrhenius equations
%Note here the Ts is converted to oF as oF is used in the original
equation from Voltz.
 kr1 = k0r1 * exp(-E1_R1/((1.8*Ts+32)+460));
 kr2 = k0r2 * exp(-E2_R2/((1.8*Ts+32)+460));
 ka1 = k0a1 * exp(-E3_R3/((1.8*Ts+32)+460));
 ka2 = k0a2 * exp(-E4_R4/((1.8*Ts+32)+460));
 ka3 = k0a3 * exp(-E5_R5/((1.8*Ts+32)+460));
 ka4 = k0a4 * exp(-E6_R6/((1.8*Ts+32)+460));
 t=0;
%UCAT tests at space velocity 20 s-1, which corresponds to time 0.05
seconds
 while t<0.05
 %BigR is defined to account for inhibition effects due to
 %chemisorption of CO and HC
 %The last term in the expression accounts for the inhibition effect of
 %NO on both oxidation rates
    BigR = (1+ ka1* CO + ka2*HC)^2 *(1+ka3*(CO*HC)^2)*(1+ka4*(NO)^.7);
    %Rate equations: krn is rate constants and BigR includes inhibition
 %effect of CO, CH and NO
    rCO = - kr1 * CO* O2/BigR;
    rHC = - kr2 * HC* O2/BigR;
 %Instantaneous concentration of CO and HC is adjusted.
    CO_new = CO + rCO * 0.0001;
    HC_new = HC + rHC * 0.0001;
 %O2 concentration can also be adjusted using the equation below as O2
is consumed mainly in oxidation of CO
    O2_new = O2 + 0.5*rCO*0.0001;
 %Percentage conversion calculation
   conversion_HC = (HCi-HC_new) / HCi *100;
   conversion_CO = (COi-CO_new) / COi *100;
 %Assign instantaneous new value to present concentration and repeat
loop
    CO=CO_new;
    HC = HC_new;
    O2=O2_new;
    t=t+0.0001;
 end
 %Store percent conversion values at each temperature in to a matrix
 conv(i) = conversion_CO;
  i=i+1;
end
 % Load data file for experimentally measured reactant conversion
across temperature range of interest
   load CoAl_CO.txt;
   Temp = CoAl_CO(1:8,1)';
   PCCO = CoAl_CO(1:8,2)';
 %Calculate errors between predicted and experimental measurement and
sum errors at all temperatures
   Error(m)= sum(abs(PCCO-conv));
 %Note here error can also be expressed in terms of percent difference
or
 %root mean square error and corresponding kinetic parameters can be
 %determined
```

```
 end
%Find the minimum sum of absolute errors across all temperatures and
%corresponding kinetic parameters
   [M,I]= min(Error)
   k = step*(I)+kr0
```

Appendix F. Differential Equations for Optimization.

$$\frac{dy(1)}{dt} = \frac{-k_0 r_1 \times e^{\frac{-E_1 R_1}{T_s+460}} \times y(1) \times y(3)}{[1 + y(1)(k_0 a_1 \times e^{\frac{E_3 R_3}{T_s+460}}) + y(2)(k_0 a_2 \times e^{\frac{E_4 R_4}{T_s+460}})]^2 [1 + (k_0 a_3 \times e^{\frac{E_5 R_5}{T_s+460}} \times y(1) \times y(2))^2][1 + k_0 a_4 \times e^{\frac{-E_6 R_6}{T_s+460}} \times (110)^{0.7}]} \quad (F1)$$

$$\frac{dy(2)}{dt} = \frac{-k_0 r_2 \times e^{\frac{-E_2 R_2}{T_s+460}} \times y(2) \times y(3)}{[1 + y(1)(k_0 a_1 \times e^{\frac{E_3 R_3}{T_s+460}}) + y(2)(k_0 a_2 \times e^{\frac{E_4 R_4}{T_s+460}})]^2 [1 + (k_0 a_3 \times e^{\frac{E_5 R_5}{T_s+460}} \times y(1) \times y(2))^2][1 + k_0 a_4 \times e^{\frac{-E_6 R_6}{T_s+460}} \times (110)^{0.7}]} \quad (F2)$$

$$\frac{dy(3)}{dt} = -0.5 \frac{dy(1)}{dt} \quad (F3)$$

Appendix G. Feasymodel Script for Voltz optimization.

```
%%% SIMPLE CHEMISTRY BOX MODEL %%%
% MCGA algorithm introduction
% Thomas Berkemeier (tberkemeier@mpic.de)
% Max Planck Institute for Chemistry, Mainz
% Modified by Yi Cao, caoy@union.edu
% Union College, Chemistry and Mechanical Engineering Department
% Last update: 2015/06/02
% REACTION MECHANISM
%2CO+O2->CO2
%CnHm+(n+m)/4*O2->nCO2+m/2 H2O
% Input parameters:
%   - rate coefficients krm and kan
%   - start and stop time
%   - initial concentrations HC, CO and O2
% Output entity: concentration of HC or CO (determined by opt.dtype)
 %% CODE
function [tout,Yout] = feasymodel(inpt,opt,setnum)
global k0r1 k0r2 E1_R1 E2_R2 E3_R3 E4_R4 E5_R5 E6_R6 k0a1 k0a2 k0a3
k0a4
 %%% DECLARATION SECTION %%%
%kinetic parameters
k0r1=inpt(1);
k0r2=inpt(2);
E1_R1=inpt(3);
E2_R2=inpt(4);
E3_R3=inpt(5);
E4_R4=inpt(6);
E5_R5=inpt(7);
E6_R6=inpt(8);
k0a1=inpt(9);
k0a2=inpt(10);
k0a3=inpt(11);
k0a4=inpt(12);
%model options
start=inpt(13);
stop=inpt(14);
%experimental conditions
CO=inpt(15);
HC=inpt(16);
OO=inpt(17);
%defining initial conditions of differential equations
y0(1)=CO;
y0(2)=HC;
y0(3)=OO;
%error tolerances
AbsTol=1e8;
RelTol=1e4;
%defining model time
t=linspace(start,stop,99);
%solving the differential equations provided in external function
options = odeset('AbsTol',AbsTol,'RelTol',RelTol);
[tout,Y] = ode23tb(@fDIFEQS,t,y0,options);
%extracting output
for j=1:opt.dtypenum(setnum)
```

```
    if strcmp(opt.dtype{j,setnum},'CO') == 1
        Yout=Y(:,1);
    elseif strcmp(opt.dtype{j,setnum},'HC') == 1
        Yout=Y(:,2);
    elseif strcmp(opt.dtype{j,setnum},'OO') == 1
        Yout=Y(:,3);
    end
end
return
% DIFFERENTIAL EQUATIONS
%rCO = - kr1 * CO* O2/BigR;
%rHC = - kr2 * HC* O2/BigR;
% d[A]/dt = - k1[A][B] - k2[A][C]
% d[B]/dt = - k1[A][B]
% d[C]/dt = k1[A][B] + k2[A][C]
function dydt = fDIFEQS(~,y)
%  k0a1 = 6.55*10^(-1);
%  k0a2 = 2.08*10^(-3);
%  k0a3 = 3.98*10^(-16);
%  k0a4 = 3.02*10^(1);
%  E1_R1 = 22600;
%  E2_R2 = 26200;
%  E3_R3 = -1730;
%  E4_R4 = -650;
%  E5_R5 = -20900;
%  E6_R6 = 6720;
global k0r1 k0r2 E1_R1 E2_R2 E3_R3 E4_R4 E5_R5 E6_R6 k0a1 k0a2 k0a3
k0a4
Ts = 550;
 %The catalyst temperature in Voltz experiment was 550 F.
%initializing vector
dydt = zeros(3,1);
%differential equations
%Rate equations: krn is rate constants and BigR includes inhibition
%effect of CO, CH and NO
%rCO = - kr1 * CO* O2/BigR;
%rHC = - kr2 * HC* O2/BigR;
dydt(1) = - (k0r1* exp(-E1_R1/(Ts+460))) * y(1)* y(3)/[(1+ (k0a1 *
exp(E3_R3/(Ts+460)))* y(1) + (k0a2 * exp(E4_R4/(Ts+460)))*y(2))^2
*(1+(k0a3 * exp(E5_R5/(Ts+460)))*(y(1)*y(2))^2)*(1+(k0a4 * exp(-
E6_R6/(Ts+460)))*(110)^.7)];
dydt(2) = - (k0r2* exp(-E2_R2/(Ts+460)))*y(2)*y(3)/[(1+ (k0a1 *
exp(E3_R3/(Ts+460)))* y(1) + (k0a2 * exp(E4_R4/(Ts+460)))*y(2))^2
*(1+(k0a3 * exp(E5_R5/(Ts+460)))*(y(1)*y(2))^2)*(1+(k0a4 * exp(-
E6_R6/(Ts+460)))*(110)^.7)];
dydt(3) = - 0.5*dydt(1);
return
```

Appendix H. Excel Spreadsheet for Voltz Optimization.

	Model name (opt.mod)		**parameter count** (this model version)			**data types** (of data set with most data types available)					
	feasymodel		17			1					
	Input parameters (INPUT)*										
			data set 1	*data set 2*	*data set 3*	*data set 4*	*: Leave arbitrary (e.g. "0") when variation bounds are given below …				
INPUT	k0r1		0	0	0	0	rate coefficient R1				
	k0r2		0	0	0	0	rate coefficient R2				
	E1_R1		0	0	0	0	exponent R1				
	E2_R2		0	0	0	0	exponent R2				
	E3_R3		0	0	0	0					
	E4_R4		0	0	0	0					
	E5_R5		0	0	0	0					
	E6_R6		0	0	0	0					
	k0a1		0	0	0	0					
	k0a2		0	0	0	0					
	k0a3		0	0	0	0					
	k0a4		0	0	0	0					
	start [s]		0	0	0	0	start time of model simulation				
	stop [s]		0.6	0.7	0.3	0.4	stop time of model simulation				
	CO0		4.00E+00	4.00E+00	7.00E-01	7.00E-01	initial concentration species A				
	HC0		5.00E+02	5.00E+02	3.00E+02	3.00E+02	initial concentration species B				
	OO0		4.50E+00	4.50E+00	3.00E+00	3.00E+00					
	fhandle2		CO0 = 4	HC0 = 500	CO0=0.7	HC0 = 300	name of data set				
					number of fitted parameters						
	KM-SUB varied kinetic input parameter ranges (bounds)**				**12**						
						MULTI ***					
			LB	UB		*data set 1*	*data set 2*	*data set 1*	*data set 2*		
BOUNDS	**k0r1**		1.60E+12	2.00E+12		1	1	1	1		
	k0r2		3.60E+13	4.00E+13		1	1	1	1		
	E1_R1		2.00E+04	2.60E+04		1	1	1	1		
	E2_R2		2.40E+04	3.00E+04		1	1	1	1		

	E3_R3		1.50E+03	2.00E+03		1	1	1	1		
	E4_R4		4.00E+02	8.00E+02		1	1	1	1		
	E5_R5		1.80E+04	3.00E+04		1	1	1	1		
	E6_R6		5.00E+03	8.00E+03		1	1	1	1		
	k0a1		4.00E-01	9.00E-01		1	1	1	1		
	k0a2		5.00E-04	4.00E-03		1	1	1	1		
	k0a3		3.00E-16	5.00E-16		1	1	1	1		
	k0a4		2.00E+01	5.00E+01		1	1	1	1		
	MCF parameters (MCFinput)										
MCF	**MCF.num**		2000		# Monte Carlo runs in each subrun						
	MCF.fit		200		# parameter sets transferred to genetic algorithm						
	MCF.unfit		200		# parameter sets generated randomly per subrun						
	MCF.grid		500000		grid-spacing for Monte Carlo sim						
	MCF.divide		500		# of max. Monte Carlo runs in each saving subunit						
	MCF.savenum		200		# of saved runs (at least MCF.fit)						
	GA parameters (GAinput)										
GA	**GA.gen**		300		# GA generations total						
	GA.submem		100		# parameter sets taken from subpopulation in each subrun						
	GA.sub		1		# subpopulations						
	GA.subgen		50		# GA generations before shake						
	GA.fitlim		1.00E-05		fitness limit (below, GA will stop)						
	GA.tolerance		9.90E+01		acceptable fitness (below, parameter set will be accepted after GA)						
DATA	**Experimental Data** (data)****				****Important: This section can be extended for more experimental data sets. Blocks for data sets separated by empty column.						
	opt.geo		aerogel	aerogel	aerogel	aerogel					
	opt.dtypenum		1	1	1	1					
	opt.dtype(1)		CO	HC	HC	CO					

	opt.LSF(1)		absolute	absolute	absolute	absolute					
	opt.dlength(1)		14	14	17	14					
	opt.weights(1)		0.2500	0.2500	0.2500	0.2500					
	time	**value**		**time**	**value**						
	data set 1			*data set 2*			*data set 3*			*data set 4*	
	0.091	3.604		0.064	468.0		0.012	275.3		0.022	0.6145
	0.152	3.308		0.122	460.4		0.018	266.7		0.029	0.5626
	0.231	3.073		0.189	456.6		0.024	253.9		0.038	0.5183
	0.283	2.400		0.238	446.0		0.025	259.8		0.039	0.5029
	0.285	2.599		0.241	417.0		0.033	227.9		0.051	0.4034
	0.287	2.698		0.279	435.3		0.035	242.9		0.053	0.4383
	0.333	2.406		0.320	358.4		0.040	186.8		0.058	0.3087
	0.365	1.649		0.378	388.1		0.046	201.4		0.067	0.2818
	0.415	0.908		0.380	282.3		0.046	194.1		0.068	0.3486
	0.420	1.589		0.396	296.0		0.046	210.0		0.080	0.2742
	0.445	0.798		0.434	183.4		0.053	193.2		0.091	0.1679
	0.470	1.485		0.442	244.3		0.065	157.5		0.098	0.1612
	0.503	0.406		0.500	103.5		0.068	148.9		0.145	0.0464
	0.541	0.047		0.672	84.5		0.084	94.5		0.176	0.0176
							0.085	99.1			
							0.107	88.6			
							0.140	61.6			

Appendix I. Experimental Data from Voltz et al. used in Voltz Optimization (*10*)**.**

Table I.1. Data sets used in Voltz optimization with instantaneous concentration of CO and HC as a function of time.

Data Set 1		Data Set 2		Data Set 3		Data Set 4	
Time (s)	[CO] (%)	Time (s)	[HC] (ppm)	Time (s)	[CO] (%)	Time (s)	[HC] (ppm)
0.091	3.604	0.064	468.037	0.022	0.615	0.012	275.342
0.152	3.308	0.122	460.426	0.029	0.563	0.018	266.667
0.231	3.073	0.189	456.621	0.038	0.518	0.024	253.881
0.283	2.400	0.238	445.967	0.039	0.503	0.025	259.817
0.285	2.599	0.241	417.047	0.051	0.403	0.033	227.854
0.287	2.698	0.279	435.312	0.053	0.438	0.035	242.922
0.333	2.406	0.320	358.447	0.058	0.309	0.040	186.758
0.365	1.649	0.378	388.128	0.067	0.282	0.046	201.370
0.415	0.908	0.380	282.344	0.068	0.349	0.046	194.064
0.420	1.589	0.396	296.043	0.080	0.274	0.046	210.046
0.445	0.798	0.434	183.409	0.091	0.168	0.053	193.151
0.470	1.485	0.442	244.292	0.098	0.161	0.065	157.534
0.503	0.406	0.500	103.501	0.145	0.046	0.068	148.858
0.541	0.047	0.672	84.475	0.176	0.018	0.084	94.521
						0.085	99.087
						0.107	88.584
						0.140	61.644

Appendix J. Feasymodel Script for UCAT Optimization.

```
%%% SIMPLE CHEMISTRY BOX MODEL %%%
% MCGA algorithm introduction
% Thomas Berkemeier (tberkemeier@mpic.de)
% Max Planck Institute for Chemistry, Mainz
% Modified by Yi Cao, caoy@union.edu
% Union College, Chemistry and Mechanical Engineering Department
% Last update: 2015/06/02
% REACTION MECHANISM
%2CO+O2->CO2
%CnHm+(n+m)/4*O2->nCO2+m/2 H2O
% Input parameters:
%   - rate coefficients krm and kan
%   - start and stop time
%   - initial concentrations HC, CO and O2
% Output entity: concentration of HC or CO (determined by opt.dtype)
 %% CODE
function [tout,Yout] = feasymodel(inpt,opt,setnum)
global k0r1 k0r2 E1_R1 E2_R2 E3_R3 E4_R4 E5_R5 E6_R6 k0a1 k0a2 k0a3
k0a4
 %%% DECLARATION SECTION %%%
%kinetic parameters
k0r1=inpt(1);
k0r2=inpt(2);
E1_R1=inpt(3);
E2_R2=inpt(4);
E3_R3=inpt(5);
E4_R4=inpt(6);
E5_R5=inpt(7);
E6_R6=inpt(8);
k0a1=inpt(9);
k0a2=inpt(10);
k0a3=inpt(11);
k0a4=inpt(12);
%model options
start=inpt(13);
stop=inpt(14);
%experimental conditions
CO=inpt(15);
HC=inpt(16);
OO=inpt(17);
%defining initial conditions of differential equations
y0(1)=CO;
y0(2)=HC;
y0(3)=OO;
%error tolerances
AbsTol=1e8;
RelTol=1e4;
%defining model time
t=linspace(start,stop,99);
%solving the differential equations provided in external function
options = odeset('AbsTol',AbsTol,'RelTol',RelTol);
[tout,Y] = ode23tb(@fDIFEQS,t,y0,options);
%extracting output
for j=1:opt.dtypenum(setnum)
```

```
    if strcmp(opt.dtype{j,setnum},'CO') == 1
        Yout=Y(:,1);
    elseif strcmp(opt.dtype{j,setnum},'HC') == 1
        Yout=Y(:,2);
    elseif strcmp(opt.dtype{j,setnum},'OO') == 1
        Yout=Y(:,3);
    end
end
return
% DIFFERENTIAL EQUATIONS
%rCO = - kr1 * CO* O2/BigR;
%rHC = - kr2 * HC* O2/BigR;
% d[A]/dt = - k1[A][B] - k2[A][C]
% d[B]/dt = - k1[A][B]
% d[C]/dt = k1[A][B] + k2[A][C]
function dydt = fDIFEQS(~,y)
%  k0a1 = 6.55*10^(-1);
%  k0a2 = 2.08*10^(-3);
%  k0a3 = 3.98*10^(-16);
%  k0a4 = 3.02*10^(1);
%  E1_R1 = 22600;
%  E2_R2 = 26200;
%  E3_R3 = -1730;
%  E4_R4 = -650;
%  E5_R5 = -20900;
%  E6_R6 = 6720;
global k0r1 k0r2 E1_R1 E2_R2 E3_R3 E4_R4 E5_R5 E6_R6 k0a1 k0a2 k0a3
k0a4
Ts = 1112;
 %The catalyst temperature in UCAT varying space velocity experiment
was 600 C(1112 F).
%initializing vector
dydt = zeros(3,1);
%differential equations
%Rate equations: krn is rate constants and BigR includes inhibition
%effect of CO, CH and NO
%rCO = - kr1 * CO* O2/BigR;
%rHC = - kr2 * HC* O2/BigR;
dydt(1) = - (k0r1* exp(-E1_R1/(Ts+460))) * y(1)* y(3)/[(1+ (k0a1 *
exp(E3_R3/(Ts+460)))* y(1) + (k0a2 * exp(E4_R4/(Ts+460)))*y(2))^2
*(1+(k0a3 * exp(E5_R5/(Ts+460)))*(y(1)*y(2))^2)*(1+(k0a4 * exp(-
E6_R6/(Ts+460)))*(259)^.7)];
dydt(2) = - (k0r2* exp(-E2_R2/(Ts+460)))*y(2)*y(3)/[(1+ (k0a1 *
exp(E3_R3/(Ts+460)))* y(1) + (k0a2 * exp(E4_R4/(Ts+460)))*y(2))^2
*(1+(k0a3 * exp(E5_R5/(Ts+460)))*(y(1)*y(2))^2)*(1+(k0a4 * exp(-
E6_R6/(Ts+460)))*(259)^.7)];
dydt(3) = - 0.5*dydt(1);
return
```

Appendix K. Excel Spreadsheet for UCAT Optimization.

	Model name (opt.mod)		**parameter count** (this model version)			**data types** (of data set with most data types available)		
	feasymodel		17			1		
	Input parameters (INPUT)*							
			data set 1	*data set 2*	*: Leave arbitrary (e.g. "0") when variation bounds are given below …			
INPUT	k0r1		0	0				
	k0r2		0	0				
	E1_R1		0	0				
	E2_R2		0	0				
	E3_R3		0	0				
	E4_R4		0	0				
	E5_R5		0	0				
	E6_R6		0	0				
	k0a1		0	0				
	k0a2		0	0				
	k0a3		0	0				
	k0a4		0	0				
	start [s]		0	0	start time of model simulation			
	stop [s]		0.6	0.6	stop time of model simulation			
	CO0		5.20E-01	5.20E-01	initial concentration species A			
	HC0		2.13E+02	2.13E+02	initial concentration species B			
	OO0		3.45E-01	3.45E-01	start time of model simulation			
					stop time of model simulation			
	fhandle2		CO0 = .52	HC0 = 212.67			name of data set	
					number of fitted parameters			
	KM-SUB varied kinetic input parameter ranges (bounds)**				**12**			
			LB	UB	MULTI ***	MULTI ***		
BOUNDS	**k0r1**		1.00E+05	1.00E+15	*data set 1*	*data set 2*		
	k0r2		1.00E+05	1.00E+15	1	1		
	E1_R1		1.00E+01	1.00E+07	1	1		
	E2_R2		3.00E+01	3.00E+06	1	1		
	E3_R3		1.00E+00	1.00E+06	1	1		

	E4_R4		1.00E+00	1.00E+06	1	1		
	E5_R5		1.00E+01	1.00E+07	1	1		
	E6_R6		1.00E+00	1.00E+06	1	1		
	k0a1		1.00E-07	1.00E-01	1	1		
	k0a2		1.00E-07	1.00E-01		1		
	k0a3		1.00E-21	1.00E-14		1		
	k0a4		1.00E+00	1.00E+06		1		
	MCF parameters (MCFinput)							
MCF	**MCF.num**		2000		# Monte Carlo runs in each subrun			
	MCF.fit		200		# parameter sets transferred to genetic algorithm			
	MCF.unfit		200		# parameter sets generated randomly per subrun			
	MCF.grid		500000		grid-spacing for Monte Carlo sim			
	MCF.divide		500		# of max. Monte Carlo runs in each saving subunit			
	MCF.savenum		200		# of saved runs (at least MCF.fit)			
	GA parameters (GAinput)							
GA	**GA.gen**		300		# GA generations total			
	GA.submem		100		# parameter sets taken from subpopulation in each subrun			
	GA.sub		1		# subpopulations			
	GA.subgen		50		# GA generations before shake			
	GA.fitlim		1.00E-05		fitness limit (below, GA will stop)			
	GA.tolerance		9.90E+01		acceptable fitness (below, parameter set will be accepted after GA)			
DATA	**Experimental Data** (data)****				*****Important: This section can be extended for more experimental data sets. Blocks for data sets separated by empty column.*			
	opt.geo		aerogel	aerogel				
	opt.dtypenum		1	1				
	opt.dtype (1)		CO	HC				
	opt.LSF(1)		absolute	absolute				

	opt.dlength(1)		7	23				
	opt.weights(1)		0.5000	0.5000				
	time	**value**		**time**	**value**			
	data set 1			*data set 2*				
	0.027	0.23		0.027	96			
	0.030	0.22		0.029	90			
	0.034	0.21		0.031	84			
	0.040	0.2		0.033	82			
	0.043	0.19		0.034	78			
	0.048	0.18		0.036	76			
	0.050	0.17		0.037	74			
				0.038	72			
				0.040	66			
				0.042	64			
				0.044	60			
				0.048	58			
				0.050	56			
				0.051	54			
				0.053	52			
				0.054	50			
				0.057	46			
				0.059	44			
				0.061	42			
				0.063	40			
				0.066	38			
				0.067	34			
				0.069	32			